J. Fluid Mech. (1988), vol. 186, pp. 163–198
Printed in Great Britain

Flow and stability of helium II between concentric cylinders

By RUSSELL J. DONNELLY AND MICHELLE M. LAMAR
Institute of Theoretical Science and Department of Physics, University of Oregon, Eugene, OR 97403, USA

(Received 17 September 1986 and in revised form 18 June 1987)

We discuss our present knowledge of the flow and stability of helium II between concentric cylinders. The flow problem for helium II leads us to consider the formation of quantized vortices in the uniform rotation of helium II in an open bucket as well as quantized circulation states and vortices in a rotating annulus. We then consider how to treat the first appearance of vortices in the presence of shear, which allows us to characterize the basic flow which must be examined for stability. The results suggest an explanation for heretofore unexplained experiments. Future directions for research on the stability of helium II are suggested.

1. Introduction

1.1. *Scope and purpose*

The stability and flow of helium II between concentric cylinders is an important and fundamental problem in fluid mechanics. It was first discussed by Chandrasekhar & Donnelly in 1957 at time when the modern theory of rotating superfluids was just beginning. Over the three decades since then there have been scattered studies, both theoretical and experimental, but it is safe to say that not much understanding of the problem has yet been achieved. The purpose of this article is to attempt to stimulate a new look at the problem.

The early work on the stability of helium II was done with rotating cylinder viscometers for the same reason that early work on the classical problem was with viscometers: there was a need to clarify the nature of friction in the fluids under study, and to establish values of viscosity. A departure of the transmitted torque from its linear relationship with the angular velocity of one or other cylinder is taken as an indication of the onset of instability. The very first experiments of Mallock (1888, 1895) and Couette (1890) showed that in classical fluids there is a substantial difference in stability between rotating the inner or outer cylinder, with the latter arrangement being much more stable. We shall show that experiments by Donnelly (1959) and Heikkila & Hollis Hallett (1955) reveal that the extra stability of flow with the outer cylinder rotating found in the classical flow is not realized in helium II, and that the underlying mechanism for this instability needs to be understood. Other studies in helium II have been undertaken using second-sound absorption, which is a powerful tool for the detection of quantized vortices.

On the theoretical side, the stability of the flow can be discussed only if the unperturbed flow is understood. Chandrasekhar & Donnelly (1957) and others since have assumed that the quantized vortices in the flow are dense enough to form a continuum. We shall examine the conditions for entry of vortices between concentric cylinders, a subject which has not previously been addressed except in the case of uniform rotation. The technique used, the minimization of a certain free energy, has always been considered inapplicable in the presence of a shear flow. We shall demonstrate that it may, after all, be possible to use free-energy minimization owing to the special circumstances of the nature of Couette flow, that is, a combination of solid-body rotation and potential flow.

The paper concludes with a discussion of future directions for research in this field. An early draft of this manuscript has stimulated some new studies which we shall describe briefly.

1.2. *Basic relationships and linear stability theory*

The coordinates for studying our problem are shown in figure 1. R_1 is the radius of the inner cylinder, R_2 the radius of the outer cylinder, and r is the distance to an arbitrary radius. The gap $d = R_2 - R_1$, and the angular velocities of the cylinders are Ω_1 and Ω_2. The ratio of the length of the apparatus L to the gap width d is called the aspect ratio,

$$\Gamma = L/d, \tag{1.1}$$

where L may exceed the length h of one cylinder if guard cylinders are present. For a classical fluid in laminar flow the velocity distribution for infinite cylinders rotating at angular velocities Ω_1 and Ω_2 is

$$v = Ar + \frac{B}{r}, \tag{1.2}$$

a combination of solid-body rotation and potential flow, where

$$A = \frac{R_2^2 \Omega_2 - R_1^2 \Omega_1}{R_2^2 - R_1^2} = -\Omega_1 \frac{\eta^2 - \mu}{1-\eta^2} \tag{1.3}$$

and

$$B = -\frac{R_1^2 R_2^2 (\Omega_2 - \Omega_1)}{R_2^2 - R_1^2} = \Omega_1 \frac{R_1^2(1-\mu)}{1-\eta^2}, \tag{1.4}$$

where

$$\mu = \frac{\Omega_2}{\Omega_1}, \quad \eta = \frac{R_1}{R_2}. \tag{1.5}$$

The vorticity ω for this flow is given by curl $\boldsymbol{v}$:

$$\omega = 2A = \frac{2[R_2^2 \Omega_2 - R_1^2 \Omega_1]}{R_2^2 - R_1^2}. \tag{1.6}$$

The torque G transmitted to a length h of one cylinder as a result of rotation of the other is given by

$$G = \frac{4\pi\eta R_1^2 R_2^2 h(\Omega_1 - \Omega_2)}{R_2^2 - R_1^2}, \tag{1.7}$$

where h is the length of the suspended cylinder and η is the viscosity of the fluid.

The problem of the stability of viscous flow between concentric cylinders was first worked out by G. I. Taylor in 1923 in a well-known paper. Taylor's work has attracted an enormous amount of interest in the 64 years since it appeared.

The stability diagram for classical Couette flow with cylinders rotating in the same direction is shown in figure 2. The solid line shows the location of the onset of Taylor vortices and secondary flow. The upper dashed line corresponds to the location of potential flow, $\Omega_1/\Omega_2 = R_2^2/R_1^2$, and the lower dash-dot line corresponds to solid-body rotation $\Omega_1 = \Omega_2$.

The potential-flow line also corresponds to the so-called Rayleigh criterion (cf. Chandrasekhar 1961) for the stability of an inviscid fluid which has the viscous fluid

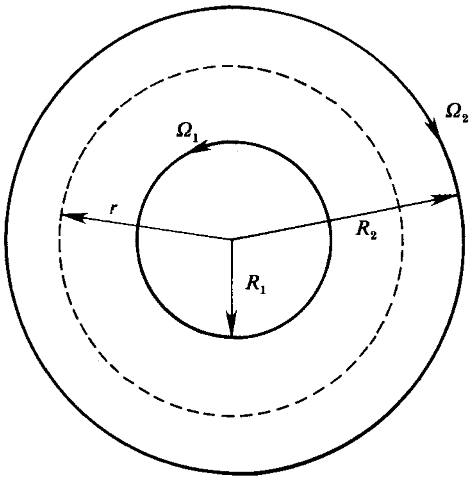

FIGURE 1. Notation for discussion of flow between concentric cylinders.

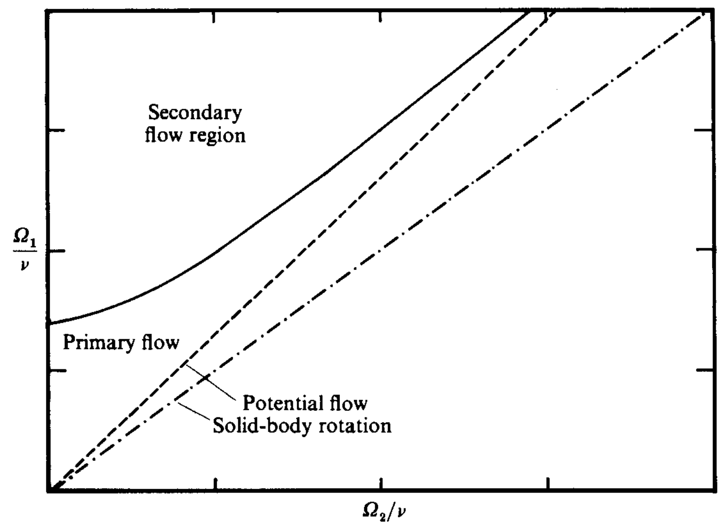

FIGURE 2. Stability diagram for cylinders rotating in the same direction (schematic only).

velocity distribution (equation (1.2)). Rayleigh's criterion for instability, $A \geqslant 0$, predicts that the flow should be stable below the dashed line and unstable above it. The difference between the solid line and the dashed line is the effect of viscosity on the stability of the flow. Note that the experimental results approach the Rayleigh criterion for large Reynolds numbers, as might be anticipated (see figures 10 and 12 of Donnelly & Fultz 1960). The vortices which arise in unstable flow are very rich and complicated in structure, as can be appreciated from the data shown in figure 3.

The Reynolds number and Taylor number of rotating-cylinder experiments have a number of definitions depending somewhat on radius ratio and personal preference (for details see Chandrasekhar 1961). We shall be referring here mostly to narrow-gap experiments, where the Reynolds number can be defined as

$$Re = \frac{\Omega_1 R_1 d}{\nu} \tag{1.8}$$

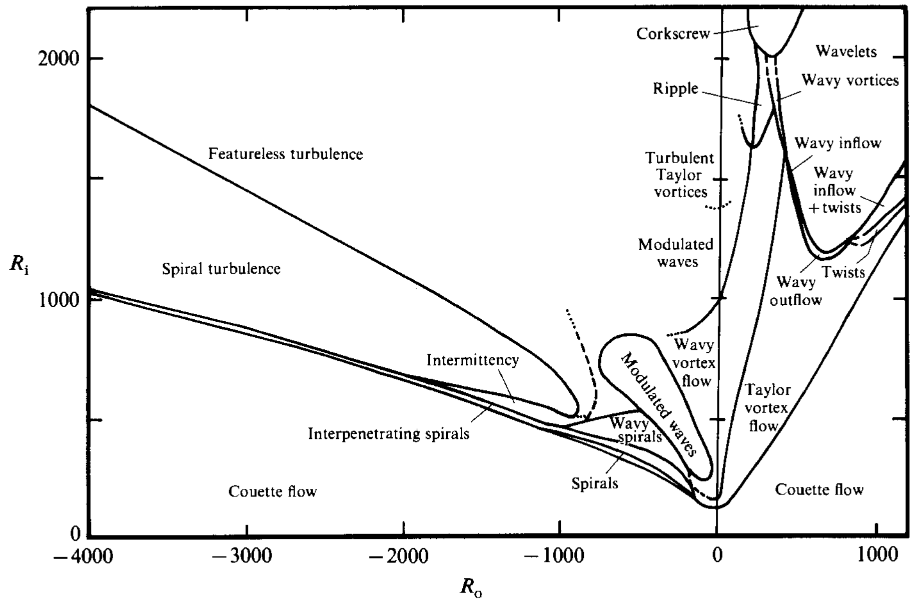

FIGURE 3. Stability diagram by Andereck, Liu & Swinney (1984) showing the astonishing variety of vortex motion which occurs in the flow between concentric cylinders. Here $\eta = 0.85$.

with the subscript 1 replaced by 2 if the outer cylinder rotates, and the Taylor number as

$$Ta = 2R_1 d^3 \left(\frac{\Omega_1}{\nu}\right)^2, \tag{1.9}$$

assuming only the inner cylinder rotates. Critical values of these parameters are denoted as Re_c and Ta_c. For helium II we shall use the dimensionless group $D_1 = \Omega_1 R_1^2/\kappa$, with D_2 defined similarly with Ω_2 and R_2. Here $\kappa = \mathrm{h}/m$ is the quantum of circulation of the superfluid, h is Planck's constant and m is the mass of the ^{4}He atom, $\kappa \sim 9.97 \times 10^{-4}$ cm^2/s.

1.3. *Precise determination of stability limits: the problem of end conditions and aspect ratio*

Before beginning the discussion of the helium II problem it is worth recalling briefly some lessons learned in classical Taylor–Couette experiments. The determination of the critical Reynolds number for the onset of an instability has proven to be a considerably greater challenge than was at first believed. One of the principal problems is the time it takes a vortex array to adjust to a change of conditions. Snyder (1969) was the first to make an estimate of the time involved. He suggested that for an apparatus of length L, the time for regularization of Taylor vortices should be $\tau_s \approx 0.15L^2/\nu$. This is a very long waiting time for water (for example) in an apparatus of even modest dimensions: for $L = 30$ cm, $\nu = 10^{-2}$ cm^2/s, $\tau_s \approx 1.35 \times 10^4$ s ≈ 3.75 hours! This result, which was not appreciated for about 10 years after it appeared, eventually encouraged investigators to re-examine the conditions for equilibrium in their apparatus, and the protocol for ramping the Reynold's number from one value to another.

Finite annulus effects have been discussed by Di Prima & Swinney (1981) in §6.6 of their review. They observe that, theoretically, the effect of the ends of the apparatus is to change the bifurcation to Taylor vortices to a continuous transition.

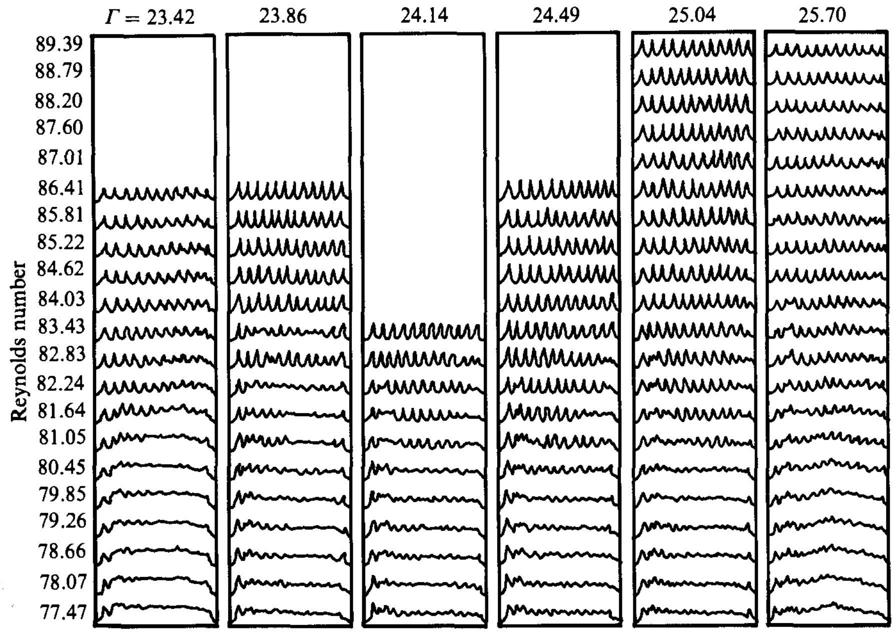

FIGURE 4. Vortex intensity plots obtained by the laser scanning method (Park & Donnelly 1981). The six data panels are for aspect ratios $\Gamma = 23.42$ to 25.70 as indicated across the top. Each trace, taken at the Reynolds number indicated on the left, shows the light reflectance beginning at the top plug on the left and ending at the bottom plug on the right. Minima in the reflectance correspond to inflowing fluid. The vortex flow for aspect ratio $\Gamma = 24.14$ sets in earlier and in a more regular manner than for other aspect ratios.

In spite of this theoretical result, it is interesting to note that some experiments still give the impression of discontinuous behaviour at the critical point. One example is the torque data of figures 4 and 7 reported by Donnelly (1958). Perhaps if these measurements were repeated with modern precautions regarding ramping rate, the torque plot would appear continuous.

Burkhalter & Koschmieder (1973) have conducted experiments varying the end conditions on the cylinders. They conclude that non-rotating end caps form the best approximation to infinite cylinder conditions.

Park & Donnelly (1981) have investigated the formation of Taylor vortices in an apparatus with varible aspect ratio so that 11–15 vortex pairs could be studied. They visualized the flow with Kalliroscope and used a vertical laser sweep to make a rapid record of all the vortex pairs in the flow (figure 4). They discovered that if there were an integral number of vortex pairs in the flow, (a multiple of the theoretical wavelength is a close estimate), the formation of Taylor vortices proceeded in a regular manner. On the other hand if such a quantization condition is not obeyed, then a dislocation might remain in the flow for some time, which although localized in the apparatus, causes the entire array of vortices to exhibit irregular, time-dependent fluctuations.

The 'experimental protocol' in a rotating cylinder experiment refers to the set of instructions given to the computer controlling the experiment. One of the most important of these instructions is the rate of increase of Ω_1, or the ramping rate. Since the controls respond to digital instructions, the ramping rate is not continuous, but occurs in discrete steps. One usually tries to use steps which are as small as possible,

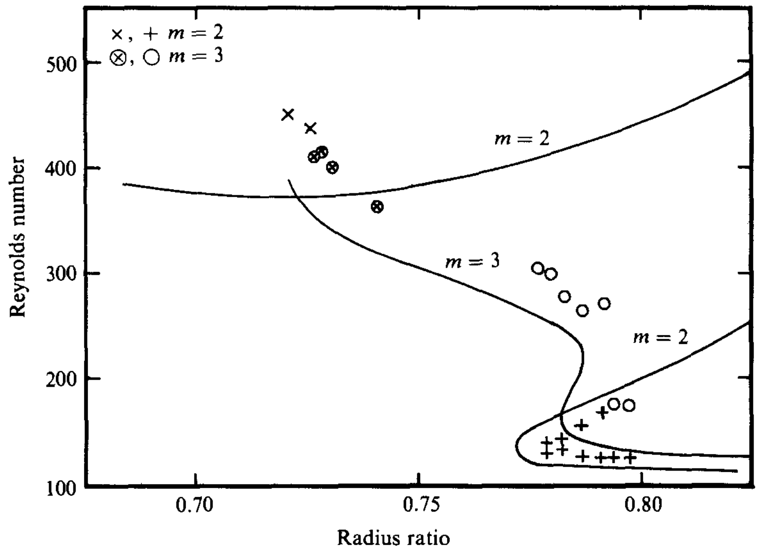

FIGURE 5. Data of Park & Jeong (1985) on the onset of the wavy modes $m = 2$ and 3 compared to calculations by Jones (1981). The unusual sensitivity to radius ratio is evident in these results. The important feature is the location of the leftmost boundaries of the $m = 2$ and $m = 3$ modes. To the left is Taylor vortex flow.

with the understanding that the steps in speed are being averaged over to give an average acceleration $a = \mathrm{d}Re/\mathrm{d}t$.

Park, Crawford & Donnelly (1981) reported an attempt to quantify how large the ramping rate a might be made by examining the vortices formed on ramping up through the onset of Taylor vortices and ramping down until the vortices disappear. They found that in order to keep hysteresis of the flow below some acceptable limit, the ramping rate $a^* = \mathrm{d}Re/\mathrm{d}t^*$ had to be kept below ~ 10, where the dimensionless time is $t^* = t/(Ld/\nu)$. This criterion suggests a somewhat more optimistic timescale than that proposed by Snyder (1969) $(0.15L^2/\nu)$. Note that the a^* criterion depends on the experiment being carried out: some experiments by Park & Jeong (1985) have had to use a^* values as low as 0.1. Furthermore, the a^* criterion was developed only for passage through the critical region. The acceptable ramping rate for highly supercritical flows has not been investigated.

When the Reynolds number is raised above the onset of Taylor vortices, it is possible to see bending waves on the Taylor vortices which travel in the azimuthal direction. This is often called the wavy vortex state of Taylor vortex flow and the number of azimuthal wavelengths is called the mode number m. These waves have amplitudes which can grow as the Reynolds number is increased and can even force vortex pairs out of the flow altogether as demonstrated by Crawford, Park & Donnelly (1985).

Expulsion, or indeed acquisition, of vortex pairs produces a radical change in the entire vortex flow and a discontinuous change in wavelength of the vortices. In another study of wavy vortices, Donnelly *et al.* (1980) showed that in an apparatus with $\eta = 0.88$ there develop turbators, i.e. dislocations in the vortex structures disturbing the entire flow, which are apparently stable in certain ranges of Reynolds numbers. These ranges of persistent turbator motion are known to depend on the ramping rate a^* and can, with sufficiently small a^*, be made to disappear entirely

(Jeong 1986). The transition to the wavy vortex state can excite different azimuthal modes m. It has been known for some time that the values of m are quite sensitive to the radius ratio η. Just how sensitive has recently been demonstrated experimentally by Park & Jeong (1985) and theoretically by Jones (1981). We reproduce the results of these authors in figure 5 to show this sensitivity.

Extensive visual studies of vortices in cylinders of small aspect ratio have been reported by Benjamin (1978*a*, *b*), by Benjamin & Mullin (1981), by Mullin (1982) and Benjamin & Mullin (1982). Here a whole range of interesting new behaviour occurs. For our purposes one of the most important results is the multiplicity of flows which can be established in the Taylor experiment. Spectacular photographs are shown by Benjamin & Mullin (1982) of fifteen different flows produced under identical conditions with $\eta = 0.600$, $\Gamma = 12.61$, $Re = 359$, $\mu = 0$.

We have cited the experiments above to demonstrate that even in the classical Taylor–Couette problem, there are difficulties and complications which require great care in preparing the flow if reproducible results are to be obtained. Little of this knowledge was available when most of the experiments in helium II discussed here were performed.

2. Early history of the flow of helium II between concentric cylinders

In this brief section we describe the three earliest experiments on rotating cylinder flow of helium II. Background on the properties of helium II is contained in many references, including a recent article on turbulent vortices (Donnelly & Swanson 1986).

2.1. *Experiments of Kapitza*

The study of helium II between rotating cylinders was begun by Kapitza (1941) who built a glass capillary tube with a concentric solid rod inside, the annular space between the pair being filled with helium II (see figure 6). When the heater is turned on, a counterflow is established in which the superfluid moves in potential flow toward the heater and the normal fluid counterflows toward the exit. The mass flux $j = \rho_n \boldsymbol{v}_n + \rho_s \boldsymbol{v}_s = 0$, where ρ_n and ρ_s are the normal and superfluid densities, $\boldsymbol{v}_n$ and $\boldsymbol{v}_s$ the normal and superfluid velocities. It was found possible to affect the transport of heat in helium II in a capillary by setting the helium into rotational motion. The heat transport was measured in a capillary (labelled 1 in figure 6) of length 4 cm and internal diameter 0.62 mm. A rod labelled 2, 0.5 mm in diameter, is rotated at speeds up to 1900 r.p.m. Control experiments established that rotation of the rod with no heat flux produces no increase of temperature inside the vessels.

The experiment was conducted by turning on the heater and measuring the temperature difference ΔT between the bulb and bath. The rod was then started into rotation and the temperature differences were observed to increase as shown in figure 7. The initial flow was subcritical (i.e. free of quantized vortices) apparently only at 2.02 K, as evidenced by a short region of zero temperature difference. The flows at 1.66 K and 1.86 K apparently were above critical before rotation was begun. The basic flow of the normal component in this experiment without rotation is axial, and with rotation, spiral.

Kapitza also measured the counterflow heat transport across a capillary with an accompanying mass flow, and found a reduction in heat transport for this flow as well. We know of no further investigation on spiral flow in helium II, but there is a considerable literature on combined heat and mass flow, summarized by Tough

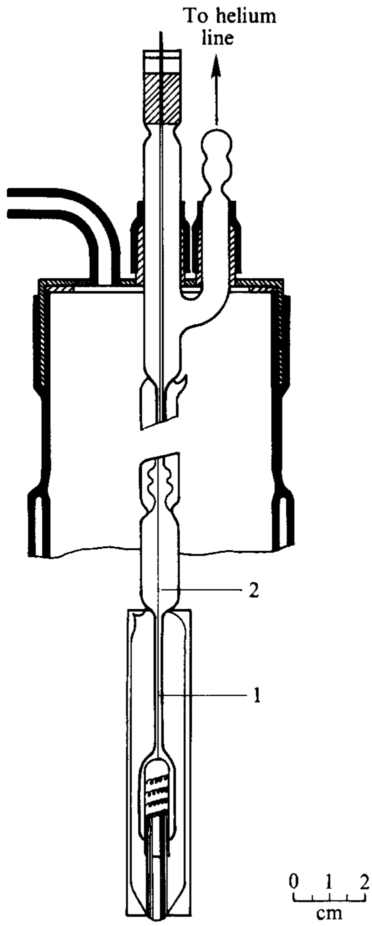

FIGURE 6. Kapitza's apparatus (Kapitza 1941). The bottom chamber, containing a heater and thermometer, is connected through capillary 1 to the bath (not shown). Rod 2 is connected through a seal at the top of the apparatus and can be rotated from the outside.

(1982) (see also Donnelly & Swanson 1986). This system deserves to be re-examined with modern techniques.

2.2. *Experiment of Hollis Hallett*

The next appearance of rotating cylinders in low-temperature physics was an apparatus built at Cambridge by Hollis Hallett (1953) who was concerned with the determination of the viscosity of helium II. The Poiseuille flow method of determining viscosity was known to yield zero viscosity under low-velocity conditions, whereas oscillating disk viscometers gave a finite viscosity. The damping of an oscillating disk at low amplitudes, however, is proportional to the product $\eta\rho_n$ where η is the viscosity and ρ_n the normal density. Values of ρ_n were just beginning to be available at that time from the Andronikashvili pile of disks experiment and second-sound velocities. Recognizing that a rotating viscometer gives one of the most direct determinations of viscosity, Hollis Hallett designed a viscometer with the outer cylinder rotating and the inner cylinder suspended by a torsion fibre.

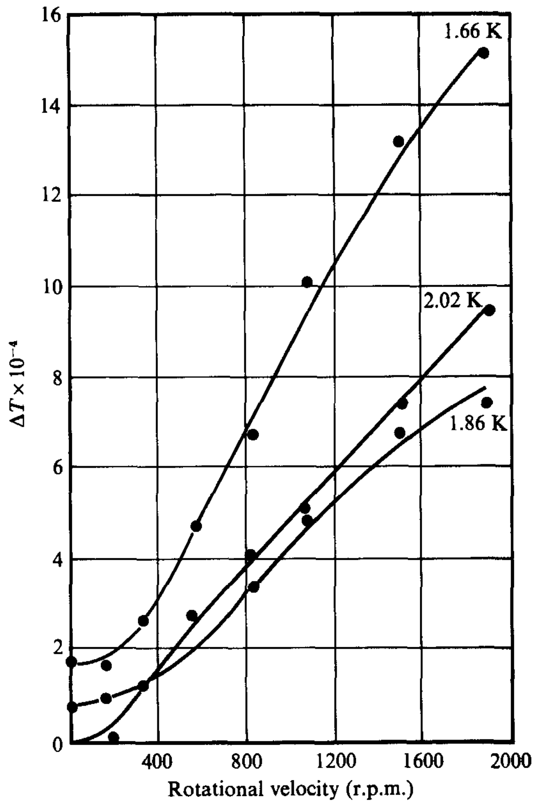

FIGURE 7. Kapitza's results, showing the increase of temperature drop across the rod and capillary as a function of rate of rotation at different temperatures (Kapitza 1941).

The apparatus had cylinders of radii $R_1 = 1.9913 \pm 0.0001$ cm, $R_2 = 2.0970 \pm 0.0006$ cm. The outer cylinder was connected to the drive shaft by means of the gear system. The inner cylinder, made of duraluminum had length $h = 2.990 \pm 0.005$ cm and was protected from end effects by guard rings. The inner cylinder was suspended by a quartz rod equipped with a magnetic damping device to control the swings of the suspended cylinder. Hollis Hallett found that in liquid helium II, the torque–rotation curve was nonlinear. As it turned out, this instrument lacked the resolution to find the laminar flow regime. Hollis Hallett continued to work with the same instrument in Toronto, as we shall describe in §4.2.

2.3. *Experiment of Wheeler, Blakewood & Lane*

Second sound in helium II is a periodic counterflow of the normal and superfluids which corresponds to temperature fluctuations rather than pressure fluctuations, as in ordinary (first) sound. The oscillating normal-fluid component in second sound has a strong interaction with quantized vortices giving rise to a force called 'mutual friction'. Mutual friction attenuates second sound and is the most sensitive method for measuring the presence of quantized vortices. All this was unknown to Wheeler, Blakewood & Lane (1955*a*, *b*) who measured the propagation of d.c. second-sound pulses in the space between concentric cylinders with the inner cylinder rotating (figure 8). Their experiment examines the alteration of the state of helium II in a shear flow. They discovered that the velocity of second sound was unchanged, but

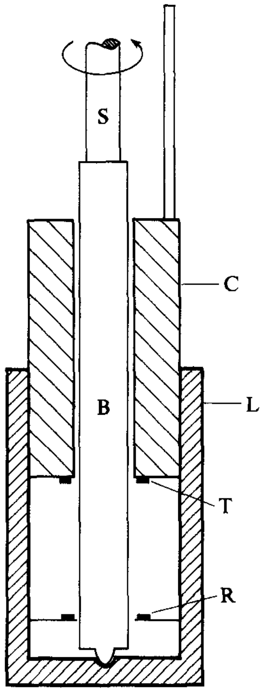

FIGURE 8. Apparatus constructed by Wheeler, Blakewood & Lane (1955*a*,*b*) to measure the attenuation of second sound between concentric cylinders, with the inner cylinder rotating. T and R are second-sound pulse transmitters and receivers. S is a drive shaft, B the inner cylinder, L the outer cylinder and C an adjustable plug.

that extra attenuation of second sound appeared. This was one of the first reports of the attenuation of second sound by quantized vortices, although strangely enough the idea of quantized vortices was not mentioned by the authors. At the end of this paper there is a reference to a paper by Hall & Vinen (1955) which reported observation of second-sound attenuation in a rotating resonator with helium II in uniform rotation, as opposed to an experiment with shear. The Hall & Vinen method, designed to study the vortex array, proved superior to the previous experiment for understanding quantized vortices and mutual friction. The Wheeler *et al.* paper, however, was the first to study the flow of helium II between concentric cylinders by second-sound attenuation.

We note here for future reference the method introduced by Hall & Vinen to determine the presence of quantized vortices in uniformly rotating helium by observing the attenuation of second sound. If a resonant mode for second sound at frequency f has a full width at half-maximum of Δ_0 and amplitude A_0 with no vortex lines present, and maximum amplitude A in the presence of vortex lines, then the attenuation of second sound is given by

$$\alpha = \frac{\pi \Delta_0}{u_2}\left(\frac{A_0}{A-1}\right), \tag{2.1}$$

where u_2 is the velocity of second sound. For the resonance, $Q = f/\Delta_0$. According to Hall & Vinen the line density expressed as length of vortex line per unit volume is given by

$$L = \frac{4 u_2 \alpha}{\kappa B}, \tag{2.2}$$

where B is a mutual friction coefficient which depends on temperature and weakly on frequency and relative velocity of the normal and superfluids (Swanson *et al.* 1987). In uniform rotation

$$L = 2\Omega/\kappa. \tag{2.3}$$

The sensitivity of this method is notable: a well-designed resonator can be used to detect quantized vortices with a least count of as little as 20 cm of quantized vortex line in a cubic centimeter of helium II. The volume of core material in such vortices is about 1 part in 10^{14} of helium II.

3. Rotation of the superfluid

In preparation for a discussion of the entry of vortices between rotating cylinders, we recall briefly earlier work on the appearance of vortices in a rotating bucket and an annulus.

3.1. *Rotation in a simple bucket*

When the original Landau model of liquid helium was first announced in the early 1940s, the normal and superfluid velocities $\boldsymbol{v}_n$ and $\boldsymbol{v}_s$ were described by two-fluid equations, and the flow of the superfluid was considered irrotational:

$$\operatorname{curl} \boldsymbol{v}_s = 0. \tag{3.1}$$

Since the two-fluid equations had predicted second sound, physicists assumed they were correct. The two fluid equations together with (3.1) predict that because only the normal fluid is rotating, the parabolic meniscus should have a depth depending on the normal-fluid fraction ρ_n/ρ. This was soon shown to be incorrect in experiments by Osborne (1950) and others. The solution of this dilemma turned out to be the hypothesis of quantization of circulation. London (1954) quotes an unpublished remark by Onsager to the effect that the superfluid will rotate in a series of concentric cylindrical shells each with azimuthal velocity $\kappa k/2\pi r$ where $k = 0, 1, 2, \ldots$. The number of rings was set by a minimization procedure. The critical velocity for appearance of a single ring of quantized circulation was

$$\Omega_c = \frac{\kappa}{4\pi R^2}, \tag{3.2}$$

where R is the radius of the bucket. This is a very low rate of rotation (8×10^{-5} rad. per s for $R = 1$ cm).

By 1955 Richard Feynman's article on vortices had appeared. Feynman realized, as Onsager did earlier (1949), the circulation in a superfluid would be quantized. But Feynman went on to suggest that in rotation the vortices would appear as lines, rather than concentric shells as had been supposed by Onsager, and the work of Hall & Vinen with second-sound attenuation has verified this idea. Feynman estimated the areal density of vortex lines by assuming that the classical vorticity

$$\omega = \operatorname{curl} \boldsymbol{v}_s \tag{3.3}$$

would be imitated by an array of vortex lines each of strength κ. Thus in a rotating bucket he predicted a density

$$n_0 = \frac{\omega}{\kappa}. \tag{3.4}$$

We refer to (3.4) as 'Feynman's rule'. Since for solid-body rotation $\omega = 2\Omega$, the predicted density is about $2000\,\Omega$ lines per cm^2. We shall show in §4.3 that (3.4) is valid for more general flows between rotating cylinders.

The difference between the Onsager proposal of concentric vortex sheets, and the Feynman vortex-line model was investigated by Hall & Vinen (see Hall 1960; Glaberson & Donnelly 1986) using the method of minimizing the free energy of the vortex array

$$F = E - \boldsymbol{M}\cdot\boldsymbol{\Omega}. \tag{3.5}$$

Here E is the energy per unit length of the vortex array and $\boldsymbol{M}$ the angular momentum. Calculations based on (3.5) shows that the vortex-line array has a lower free energy than the vortex-sheet array and hence will be preferred. The calculations also show that the vortex lines rotate with the container and that there is probably one layer of lines missing at the edge of a rotating bucket. Experiments (reviewed recently by Glaberson & Donnelly 1986) support this idea. For purposes of this discussion we shall ignore this boundary correction, although the reader should be aware that it exists and is important in some experiments. A criterion for neglecting the boundary correction is that the mean spacing between vortex lines

$$\delta = (\kappa/\omega)^{\frac{1}{2}} \tag{3.6}$$

is small compared with the radius of the bucket, or gap between cylinders.

3.2. *Rotation in an annulus: theory*

Returning to the flow between concentric cylinders, the annular-bucket problem corresponds to $\Omega_2 = \Omega_1$. The calculation of the critical velocity for the appearance of quantized circulation states and vortices in an annular region in solid-body rotation was addressed by Vinen (1961) for very small radius ratio, by Donnelly & Fetter (1966), and later more completely by Stauffer & Fetter (1968) for a narrow gap. The technique was again free-energy minimization. They showed that at low angular velocities the equilibrium superflow is a purely irrotational circulation with tangential velocity as close as possible to that of the cylinders. The quantized circulation states form a sequence of equally spaced levels up to a critical angular velocity

$$\Omega_0 = \frac{\kappa}{\pi d^2}\ln\left(\frac{2d}{\pi a}\right), \tag{3.7}$$

at which point singly quantized vortices appear in the bulk of the fluid. For Ω just beyond Ω_0 the vortices are equally spaced on a circle midway between the walls, and their number increases rapidly with Ω.

Stauffer & Fetter (1968) were also able to estimate the angular velocity for the appearance of the second row of vortices.

A further remark of Donnelly & Fetter may be useful here. They note that quantized vortices appear in the annulus at an angular velocity Ω_0 when vortices can first compensate for the difference in irrotational velocity between the inner and outer walls. This result will prove to be important for the discussion of the flow between concentric cylinders in the presence of shear: it suggests that vortices will appear in an attempt to prevent large relative velocities between the superfluid and the walls.

With these insights we shall now proceed to examine the experimental situation for flow on the solid-body-rotation line of figure 2.

3.3. *Rotation in an annulus: experiments*

Experiments to detect the appearance of the first row of vortices in an annulus with second sound were carried out by Bendt & Donnelly (1967) and reported more fully

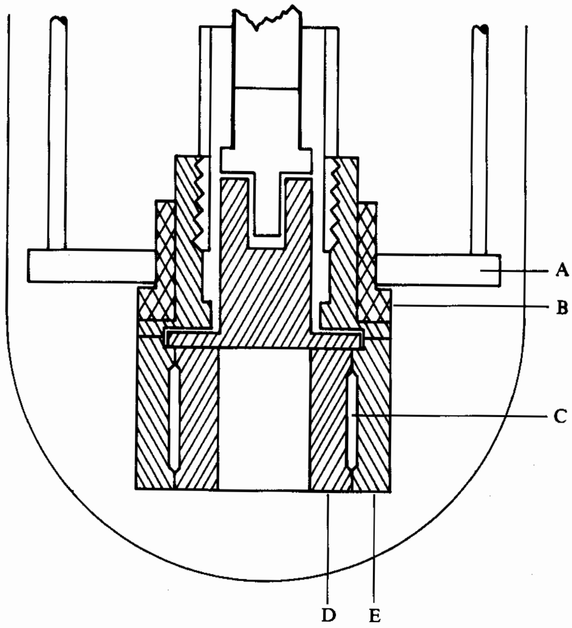

FIGURE 9. Rotation-annulus apparatus of Bendt & Donnelly (1967) and Bendt (1967*b*). The frame A is stationary, and the bearing B is machined from Kel-F plastic. The rotating resonant cavity C is formed from one of five interchangeable inner cylinders D, and a fixed outer cylinder E, all made of anodized aluminium. Second sound was generated and received by Aquadag coatings on the cylindrical walls.

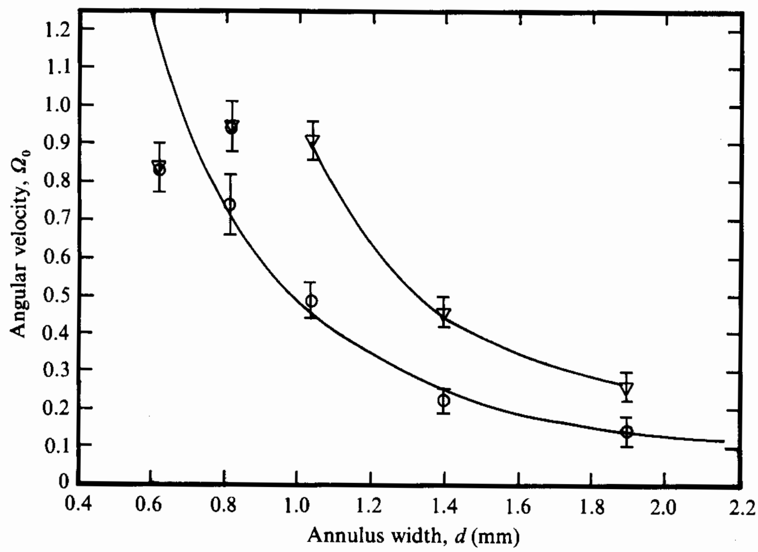

FIGURE 10. Data of Bendt (1967) showing experimental determination (circles) of Ω_0 given by Donnelly & Fetter's relationship (3.11) (the lower solid line) and 1.4 K. The second harmonic (triangles) was thought to be sensitive to the appearance of a second row of vortices, as calculated by Stauffer & Fetter (1968) (the upper solid line).

by Bendt (1967*b*). Their apparatus was an annular resonator made up of a fixed outer cylinder and five interchangeable inner cylinders (figure 9). Here $R_2 = 1.560$ cm and $d = 0.062$, 0.082, 0.104, 0.140, and 0.190 cm.

Their experimental values of Ω_0 are shown in figure 10 and it is clear that except for the narrowest gap the results are in good agreement with (3.7).

Bendt & Donnelly (1967) and Bendt (1967*b*) also measured the attenuation of second sound with a second harmonic which has a node in the middle of the annulus. If the vortices form in the middle of the gap, as predicted, then the second harmonic should be relatively insensitive to their presence. This indeed was the case: attenuation for the second harmonic first appeared at about $1.9\Omega_0$, which the authors attributed to the appearance of a second row of vortices. The appearance of a double row was predicted to be at about $1.85\Omega_0$ by Stauffer & Fetter (1968).

4. Flow of helium II between concentric cylinders

We are now in a position to discuss all the known experimental and theoretical evidence on the flow of helium II between concentric cylinders. The various measures of rotation of the cylinders are defined much as in § 1.3. For the Reynolds number and Taylor number there is clearly a question of which density, ρ or ρ_n, should be used for the kinematic viscosity. If the normal and superfluids are not coupled by mutual friction, the kinematic viscosity of the normal fluid would be $\nu_n = \eta/\rho_n$. In what follows the inner cylinder is denoted by a subscript 1 and the outer cylinder by subscript 2. The further subscript c denotes the critical values of these parameters. The classical Reynolds number is denoted by *Re*, and that for helium II is based upon the uncoupled normal fluid parameters:

$$Re_n = \frac{\Omega_1 R_1 d}{\nu_n}. \tag{4.1}$$

The corresponding Taylor number is

$$T_a = \frac{2R_1 d^3 \Omega_1^2}{\nu_n^2}, \tag{4.2}$$

where $\nu_n = \eta/\rho_n$, and the dimensionless quantum parameter

$$D_1 = \frac{\Omega_1 R_1^2}{\kappa}, \tag{4.3}$$

where these definitions can apply to rotation of either cylinder by changing subscripts.

The average number of vortices across the gap, N_v, can be estimated roughly by noting that the mean spacing between vortices is δ (cf. (3.6)) and we define

$$N_v \approx \frac{d}{\delta} = \left\{\frac{2\,|D_2 - D_1|\,d}{(R_1 + R_2)}\right\}^{\frac{1}{2}}.$$

We shall tabulate N_v at the *first* critical velocity observed in the tables of data summarizing the experiments.

We shall see that the evidence from rotating-cylinder viscometer measurements suggests that the extra stability gained by rotating the outer cylinder in classical Couette flow is not realized in helium II. The experiments of Bendt (1966, 1967*a*), described in §4.5, give useful information on the penetration of vortices between

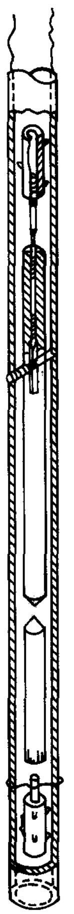

FIGURE 11. Apparatus employed by Kolm & Herlin (1956) to study the dynamics of helium II. The inner cylinder is shown suspended by Beams type of magnetic suspension. This cylinder was set into rotation and observed to coast to rest as shown in figure 12.

rotating cylinders and the relationship of the line density to the vorticity of the flow set by cylinder rotation. The torque experiments of Donnelly, the second-sound absorption experiments of Snyder and Wolfe *et al.*, and the theories of Chandrasekhar, Mamaladze & Matinyan, will also be discussed. In §4.9 we consider how to generalize the calculations of §3 above so that the entry of vortices between rotating cylinders in the presence of shear can be computed. This will be the starting point for future stability theories of helium II.

4.1. *Experiment of Kolm & Herlin*

Kolm & Herlin (1956) constructed the apparatus shown in figure 11. An iron rotor is placed inside a Plexiglas tube. The upper part of the rotor is conical in shape and is suspended below the conical top of an iron core by a magnetic field produced by a solenoid surrounding the iron core. The horizontal position of the rotor is fixed by the divergence of the axially symmetric field, and its vertical position is stabilized by a servomechanism which controls the current in the solenoid and derives its input signal from a sensing coil mounted below the rotor. The rotor was itself essentially free of friction, and the experiment consisted of accelerating the rotor to some

Apparatus dimensions	R_1 (cm)	0.635
	R_2 (cm)	0.794
	d (cm)	0.159
	h (cm)	7.62
Constants	η (μP)	20.70
	ρ_n (g/cm^3)	0.1222
Measured values	T (K)	2.135
	Ω_c (rad/s)	2
Calculated values	Re_{nc}	1192
	D_{1c}	809
	N_v	13

TABLE 1. Data of Kolm & Herlin (1956). Note that values of η and ρ_n are currently accepted magnitudes.

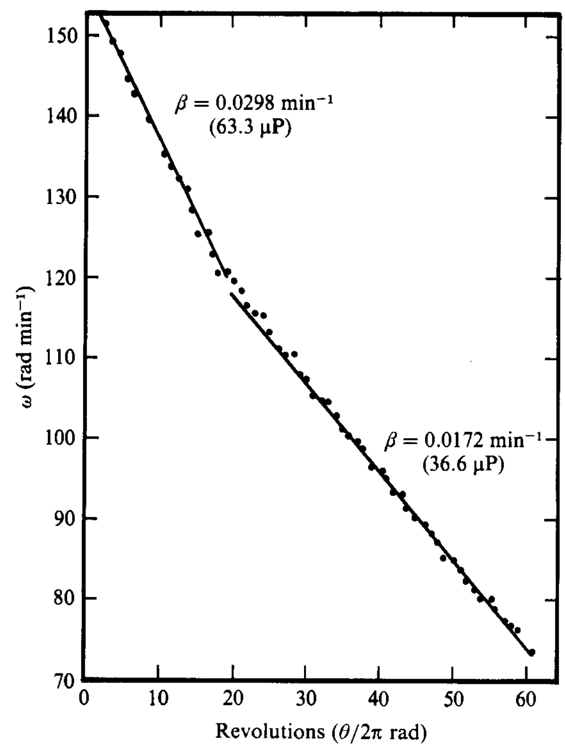

FIGURE 12. Data obtained by Kolm & Herlin (1956) at 2.135 K showing the decay of rotation rate of the rotor shown in figure 11. The slope β of the decay corresponds to the effective viscosities shown.

suitable initial velocity, and then permitting it to coast freely. The slowing of the rotor was determined by optical detection of marks on the bottom of the rotor. Apparatus dimensions and some results are shown in table 1. The authors report great difficulty with the apparatus and few results. One interesting result is shown in figure 12 where the data indicate a break in damping at about 120 rad per min, corresponding to a change in the effective viscosity of the liquid from 63.3 μP to 36.6 μP. The latter value is still about twice too high owing perhaps to some instability still present in the flow (cf. Chandrasekhar & Donnelly 1957).

Apparatus dimensions		R_1 (cm)	1.991
		R_2 (cm)	2.097
		d (cm)	0.106
		h (cm)	2.990
		Figure 13	Figure 14
Constants	η (μP)	13.04	14.81
	ρ_n (gm/cm^3)	0.0486	0.0819
Measured values	T (K)	1.82	2.002
	v_c (cm/s)	0.095	0.092
	Ω_c (rad/s)	0.0453	0.0439
Calculated values	Re_{nc}	35.6	51.2
	D_{2c}	180	174
	N_v	3.1	3.0

Observed values of the critical velocity

T (K)	v_c (cm/s)	T (K)	v_c (cm/s)
2.180	0.25?	1.496	0.085
2.100	0.09	1.400	0.070
2.002	0.093	1.308	0.080
1.820	0.095	1.250	0.080
1.650	0.055	1.131	0.12?

TABLE 2. Data of Heikkila & Hollis Hallett (1955). The outer cylinder is rotating, η and ρ_n are currently accepted magnitudes; errors on v_c are $\sim$ 10%; 2.180 K was, at the time, below T_λ.

In the light of the difficulties the authors report with their apparatus, including eddy current heating of the rotor, this type of apparatus is not likely to be of long-range use in studying helium II. The boundary conditions on the rotor ends are poorly defined, and the constant deceleration of the rotor may prevent the flow from ever reaching equilibrium. The idea of a magnetic suspension, however, is novel in Couette flow, and may be useful with more modern technology.

4.2. *Experiments of Heikkila & Hollis Hallett*

Hollis Hallett moved to the University of Toronto in the early 1950s taking the viscometer described in §2.2. There he undertook a more ambitious programme of the study of the hydrodynamics of helium II and soon was able to achieve an order-of-magnitude greater sensitivity in torque. He adopted a 15μ tungsten fibre 20 cm long as the torsion wire. Data of Heikkila & Hollis Hallett (1955) are shown in table 2.

The results of torque measurements with the outer cylinder rotating are shown in figures 13 and 14, where the solid circles are new data and the open circles data obtained at Cambridge. The values of viscosity reported by the authors, converted to the T58 temperature scale, are still useful and are discussed in the tables of Barenghi *et al.* (1987). The critical Reynold's number observed, based upon the uncoupled normal fluid parameters and the outer cylinder rotation rate, is $Re_{nc} = \Omega_{2c} R_2 d\rho_n/\eta = 51$ at 2.0 K and should be compared to Donnelly's results in §4.4 below).

4.3. *Theory of Chandrasekhar & Donnelly*

Chandrasekhar & Donnelly (1957) were the first to consider the stability of the flow of helium II between rotating cylinders. They noted that if the Landau equations of motion are used then the superfluid would obey the Rayleigh stability criterion (see

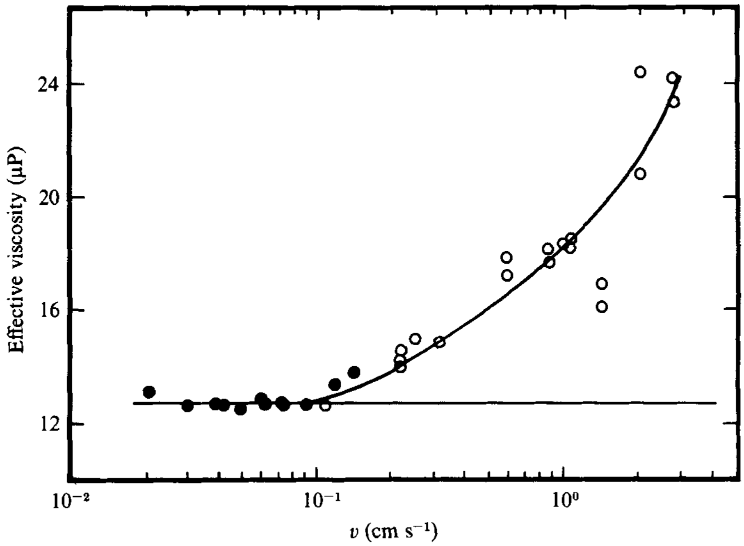

FIGURE 13. Data obtained by Heikkila & Hollis Hallett (1955) at 1.82 K using a rotating-cylinder viscometer with the outer cylinder driven. v is the velocity of the outer cylinder. The solid points are new data, the open points from the earlier report of Hollis Hallett (1953).

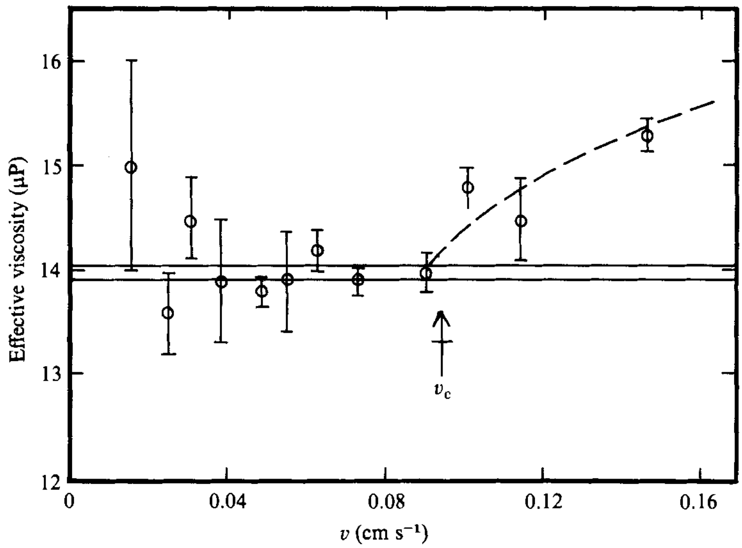

FIGURE 14. Data obtained by Heikkila & Hollis Hallett (1955) at 2.002 K showing the analysis to locate the critical velocity and the absolute viscosity. $\eta = 13.94 \pm 0.07$ μP and $v_c = 0.093 \pm$ 0.003 cm/s.

§1.2), and in particular would be unstable for any rotation of the inner cylinder. The normal fluid would act as a classical viscous fluid with viscosity ν, density ρ_n and kinematic viscosity $v_n = \eta/\rho_n$, and thus would be unstable when the Taylor number $Ta \geqslant T_c$. The authors note that when mutual friction is included the situation is drastically changed. The presence of vortex lines introduces a coupling due to mutual friction between the two fluids. The superfluid instability is raised above its value of zero for rotation of the inner cylinder and the normal-fluid instability is raised above

	Apparatus dimensions		R_2 (cm)	2.00	
			R_1 (cm)	1.90	
			d (cm)	0.1	
			h (cm)	5	
	Figure 15	(*a*)	(*b*)	(*c*)	(*d*)
Constants	η (μP)	1650	18.20	13.39	14.48
	ρ (g/cm^3)	0.81	0.1091	0.0165	0.084
Measured Values	T (K)	77	2.1	1.5	1.35
	P_n (s)	3.47	29.49	72.55	60.03
	P_s (s)	—	35.43	141.47	148.42
	Ω_1 (rad/s)	1.18	0.177	0.0444	0.0423
	Ω_2 (rad/s)	—	0.213	0.0866	0.1047
Calculated values	Re_{cn1}	169	202	10.4	4.66
	Re_{cn2}	—	243	20.3	11.5
	D_{1c1}	—	641	159	153
	D_{1c2}	—	771	313	379
	N_v	—	5.7	4.0	4.4

TABLE 3. Data of Donnelly (1958). Note that figure 15(*a*) gives data for liquid nitrogen, while (*b*), (*c*), and (*d*) are for helium II, inner cylinder rotating. Viscosities and densities are currently accepted magnitudes. For (*a*) $P_n = P_c$, $\Omega_1 = \omega_c$, and $Re_{cn1} = Re_c$.

the classical value of $Ta_c = 1708$. Numerical results are contained in table I of the paper.

The experiment of Kolm & Herlin described in §4.1 above was interpreted by Chandrasekhar & Donnelly as the unstable flow between the two critical velocities where the drag might be greater owing to disturbances from the lower branch.

The theory of Chandrasekhar & Donnelly omits a term in the equations of motion for a rotating fluid which was not appreciated at the time, namely the effect on stability of the tension in the vortex lines. This 'tension' arises because vortex lines have an energy per unit length which can be interpreted as a tension (see, for example, Glaberson & Donnelly 1986). The stability problem becomes very complicated with the full equations, but some insight may be obtained by considering a derivation equivalent to the Rayleigh criterion, as reported in §4.9 below.

4.4. *Experiments of Donnelly*

Donnelly's (1958) torque apparatus was designed to work in cryogenic as well as classical fluids. His 1959 experiments were designed to verify the ideas of Chandrasekhar & Donnelly. The deflection of the outer cylinder is denoted as ϕ and the period of rotation of the inner cylinder as P, so that in laminar flow the product ϕP is proportional to G/Ω_1 and hence is proportional to the viscosity of the fluid. The constant $C = \eta/\phi P$ was determined by calibration in air. Some data are given in table 3. The results shown in figure 15 were carried out with cylinders of radii $R_1 =$ 1.9 cm, $R_2 = 2.0$ cm. Figure 15(*a*) shows data for liquid nitrogen obtained with a slightly above atmosphere pressure to prevent bubbling. The observed viscosity, $\eta = 1.49\times10^{-3}$ P, is about right for the liquid at 77 K ($\sim 1.65\times10^{-3}$ P). The critical Reynolds number corresponding to P_c is $\sim$ 169, compared to the theoretical value for $R_1/R_2 = 0.95$ of 185, showing that the apparatus is working correctly.

Results at three temperatures in helium II are shown in figure 15(*b–d*). The torsion fibre used was considerably more sensitive than the one used for liquid nitrogen. The

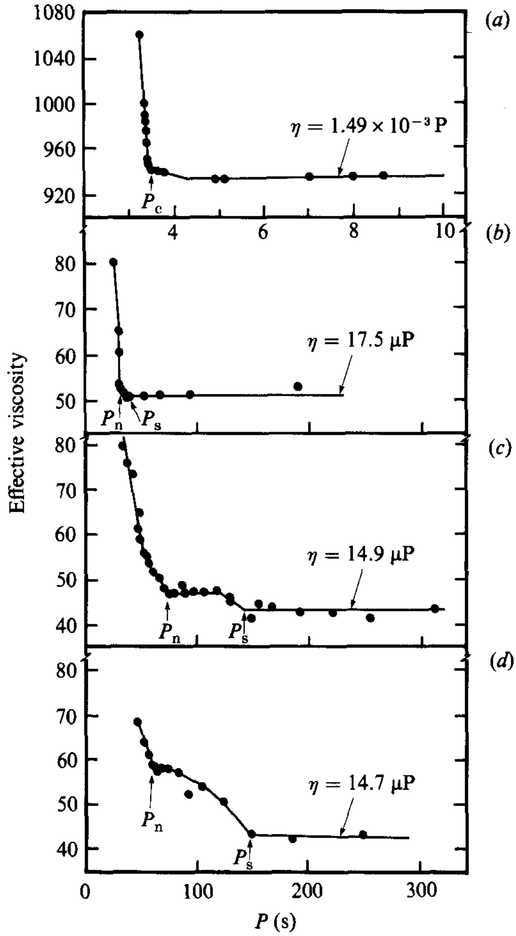

FIGURE 15. The variation of effective viscosity, proportional to ϕP, with period of rotation of the inner cylinder as obtained by Donnelly (1959). (*a*) Liquid nitrogen, 77 K, $C = 1.60 \times 10^{-6}$; (*b*), (*c*) and (*d*) liquid helium II at 2.1 K, 15 K and 1.35 K respectively, $C = 3.43 \times 10^{-7}$. P_s and P_c denote the critical periods of rotation for instability which Donnelly believed were due to instabilities in the superfluid and normal fluid as discussed by Chandrasekhar & Donnelly (1957).

viscosities obtained in the laminar flow regimes are comparable to modern estimates (18.9 μP at 2.1 K, 13.39 μP at 1.5 K and 14.48 μP at 1.35 K). At all three temperatures two discontinuities are observed in the effective viscosity relationship; the separation in these speeds widens as the temperature is lowered. (The rise in effective viscosity between P_s and P_n at 2.1 K is much larger than the rise before P_c in liquid nitrogen.) Donnelly interpreted his results as confirmation of the ideas advanced earlier by Chandrasekhar & Donnelly (1957) that two instabilities occur, one associated with the normal fluid and one with the superfluid (see §4.4).

An important point about the stability of helium II can be established by comparing the results with the earlier work of Heikkila & Hollis Hallett discussed in §4.2. These authors obtained $Re_{nc} = 51$ at 2.0 K with the outer cylinder rotating; Donnelly obtained $Re_{nc} = 202$ at 2.1 K with the inner cylinder rotating. At lower temperatures Heikkila & Hollis Hallett obtained $Re_{nc} = 3.85$ at 1.35 K and Donnelly obtained $Re_{nc} = 4.66$ at 1.35 K. Thus it appears, on the face of it, that rotation of liquid helium II near T_λ is *less* stable with the outer cylinder rotating than the inner!

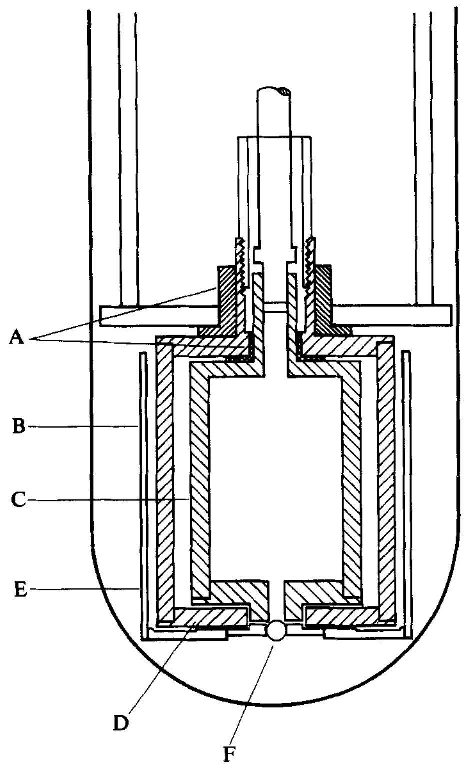

FIGURE 16. Rotating annular second-sound resonant cavity built by Bendt (1966). The bearings A are Kel-F, and the rotating cylinders are B and C. D marks the location of holes drilled in the bottom plate to release the heat generated by aquadag transducers painted on B and C. E is an aluminium shield and F a ball bearing.

And considering that Couette (1890) and Taylor (1936) obtain $Re_c \sim 2000$ for rotation of the outer cylinder, the outer-cylinder rotation is dramatically less stable than for a classical fluid.

4.5. *Bendt's Experiments*

A direct experimental test of Feynman's rule (3.4) was provided by Philip Bendt (1966, 1967*a*) in papers which we believe have been underappreciated. Bendt constructed a highly precise pair of concentric cylinders of radii $R_1 = 2.722$ cm, $R_2 = 3.333$ cm with a gap $d = 0.6105$ cm, which was reduced to $d = 0.608 \pm 0.002$ cm with aquadag coatings used for generation and detection of second sound (figure 16).

Bendt's cylinders were carefully chosen so that $(R_2/R_1)^2 = 1.50$. Thus by arranging to rotate either cylinder and by constructing a special gearing which makes $\Omega_1/\Omega_2 = 3/2$ he was able to produce four flows of different vorticity ω: (cf. (1.6))

(1) solid-body rotation, $\Omega_1 = \Omega_2$, $\omega = 2\Omega_1$;
(2) $\Omega_2 = 0$, $\omega = 4\Omega_1$;
(3) $\Omega_1 = 0$, $\omega = 6\Omega_2$;
(4) potential flow, $\Omega_1/\Omega_2 = 3/2$, $\omega = 0$.

Bendt determined the relative vortex-line density by measuring the attenuation of second sound using deposited carbon (aquadag) transducers on the insides of the cylinders. After careful checks for allowed power input and linearity of attenuation with angular velocity, he measured the radial attenuation α and hence deduced the

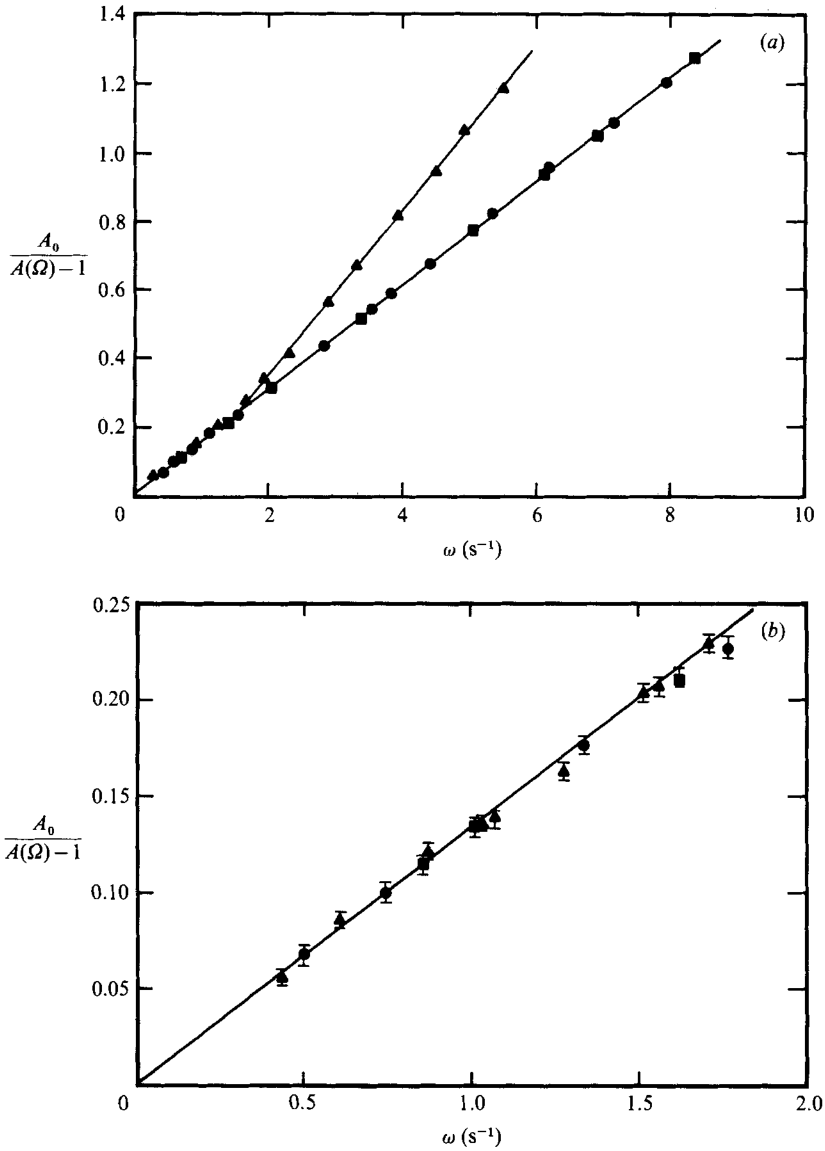

FIGURE 17. Second-sound attenuation results obtained by Bendt with the apparatus of figure 16. (*a*) Results at 1.4 K showing the excess attenuation of second sound under the indicated conditions. (*b*) Detail showing the correspondence of all results below the critical velocity when plotted against ω. This is a direct test of Feynman's rule, (3.4). ●, Solid-body rotation; ■, outside cylinder only; ▲, inside cylinder only.

mutual friction coefficient B. His values were in good agreement with earlier values and indeed agree to within 9% with contemporary accepted values (Barenghi, Donnelly & Vinen 1983).

The results are shown in figure 17 (*a*, *b*), scaled as attenuation α *vs.* vorticity ω. If the relationship (1.6) between ω and rotation rates did not hold, the collapse of data along a single line would not occur. The deviation of attenuation for the inner cylinder rotating indicates the onset of some type of secondary flow when the inner cylinder rotates faster than 0.4 rad/s.

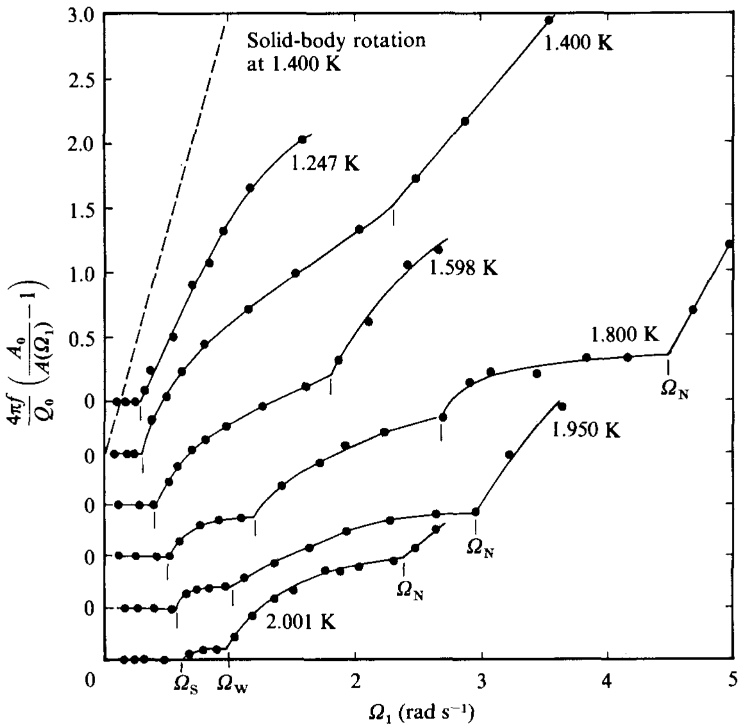

FIGURE 18. Results on the attenuation of second sound by Bendt exploring along the potential-flow line (dashed) of figure 2, $\Omega_1/\Omega_2 = R_2^2/R_1^2 = 1.500$. Theoretically vortices should not exist on this line, but are observed to enter at Ω_s.

T (K)	Ω_s (s^{-1})	D_{1c}
1.247	0.30	2230
1.400	0.32	2380
1.598	0.42	3120
1.800	0.52	3860
1.950	0.60	4460
2.001	0.63	4680

TABLE 4. Velocities at which Bendt (1966, 1967*a*) observed attenuation to begin in his experiments on potential flow. $D_{2c} = D_{1c}$; Ω_s is defined in figure 18.

For the case of potential flow, Bendt reports the data reproduced in figure 18, taken after a transient decay time of 6 or 8 min which shows that for $\Omega_1 < \Omega_s$ (see table 4) there is no observable attenuation.

Bendt's experiments establish that over his range of speeds, the superfluid adopts the classical (viscous) fluid velocity distribution, (1.2). They further establish that the vortex-line density is given by Feynman's rule, (3.4).

4.6. *Experiments of Synder*

H. A. Snyder (1974) reported the beginning of an ambitious set of experiments. His approach was to solve the Hall–Vinen–Bekarevich–Khalatnikov (HVBK) equations of motion for He II. These equations are based upon the idea of treating the vortices as a continuous distribution while recognizing the elastic properties of the vortices

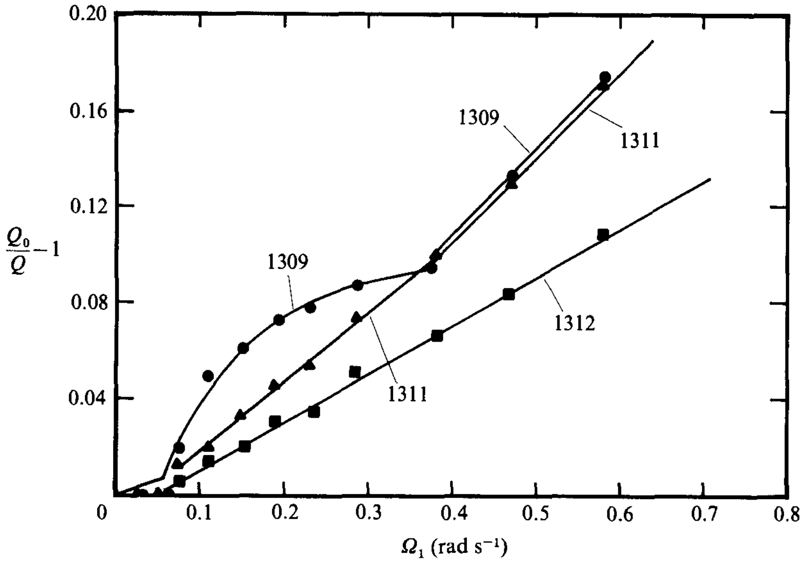

FIGURE 19. Second-sound attenuation measurements by Snyder (1974). The numbers denote the frequencies of various resonant modes. The critical angular velocities Ω_{c1} and Ω_{c2} correspond to the breaks in the 1309 Hz curve.

Apparatus dimensions	R_1 (cm)	0.795
	R_2 (cm)	1.590
	d (cm)	0.795
	h (cm)	12.04
Constants	η (μP)	13.05
Measured values	T (K)	1.63
	Ω_{c1} (rad/s)	0.07
	Ω_{c2} (rad/s)	0.38
Calculated values	Re_{nc1}	91
	Re_{nc2}	493
	D_{1c1}	44.4
	D_{1c2}	241
	N_v	5.4

TABLE 5. Data of Snyder (1974). η is based on current data. Outer cylinder is at rest.

which arise because vortices have an energy per unit length. The derivation of these equations is presented by Hall (1960). The plan was to solve the HVBK equations for linear stability similar to the approach of Chandrasekhar & Donnelly (1957). The difference he proposed was to use the HVBK equations, which were not formulated at the time Chandrasekhar & Donnelly did their work, and to use numerical methods to obtain solutions. He chose $\eta = R_1/R_2 = 1/2$.

Snyder's apparatus followed the Bearden (1939) design. Change gears were provided to allow the inner and outer cylinders to turn at fixed ratios of angular velocity. A second-sound transmitter and receiver were painted on the anodized aluminium inner cylinder. Aquadag was used as a temperature-dependent resistance for detecting second sound and the transmitter was a heater made of silver paint. Some resonant Q's (see §2.3) exceed 5000 even with the cylinders rotating, which Snyder interprets as meaning that the space between cylinders is uniform to better

		Figure 21	Figure 22
Apparatus dimensions	R_1 (cm)	2.075	2.57
	R_2 (cm)	2.65	2.65
	d (cm)	0.575	0.08
	h (cm)	9.0	9.0
Constants	η (μP)	14.6	13.2
	ρ_n (gm/cm^3)	0.0791	0.0546
Measured values	T (K)	1.99	1.86
	(rad/s)	$\Omega_1 = 0.38$	$\Omega_0 = 0.25$
	(rad/s)	$\Omega_2 = 1.07$	$\Omega_1 = 1.45$
	(rad/s)	$\Omega_3 = 2.75$	$\Omega_3 = 6.66$
	(rad/s)	$\Omega_4 = 5.65$	
Calculated values		$R_{nc1} = 2460$	$R_{nc0} = 213$
		$R_{nc2} = 6920$	$R_{nc1} = 1230$
		$R_{nc3} = 17800$	$R_{nc3} = 5660$
		$R_{nc4} = 36500$	
		$D_{1c1} = 1640$	$D_{1c0} = 1660$
		$D_{1c2} = 4620$	$D_{1c1} = 9610$
		$D_{1c3} = 11900$	$D_{1c3} = 44100$
		$D_{1c4} = 24400$	
		$N_v = 20$	$N_v = 17$

TABLE 6. Data of Wolf *et al.* (1981): the inner cylinder is rotating. η and ρ_n are currently accepted magnitudes. N_v is computed for Ω_1.

than 0.25 μm, even during rotation. In his experiment he inferred the presence of vortices by analysing the second-sound resonance curves as a function of rotation rate. Since the additional attenuation of second sound by vortex lines is dependent on the angle between the direction of wave propagation and the vortex lines, each resonant mode will react differently to a given array of vortex lines.

The data shown in figure 19 and table 5 were taken at $T = 1.63$ K with $\Omega_2 = 0$. Each mode of resonance, indicated by the corresponding resonant frequency in Hz, has a different dependence of excess attenuation on Ω_1. All the curves have some features in common. There is a range of no additional attenuation at the lowest speeds of rotation. Apparently this range is analogous to the vortex-free flow in a rotating annulus (i.e. $\Omega < \Omega_0$ in figure 10).

4.7. *Experiments of Wolf et al.*

The most recent experiments on the stability of helium II between rotating cylinders have been reported by Elleaume, Hulin & Perrin (1978), and by Wolf *et al.* (1981) see table 6. They report the first comprehensive use of second-sound attenuation as a tool to study the stability of helium II between rotating cylinders. In principle they could examine the attenuation in the azimuthal, radial and axial directions: much can be learned about vortex distributions in this manner.

Their apparatus is shown in figure 20 and consists of cylinders made of duralinox: $R_2 = 2.65$ cm, with interchangeable inner cylinders giving gaps of $d = 0.575$, 0.35, 0.15 and 0.08 cm. The length of the cylinders is $h = 9.0$ cm. The study was made by observing the attenuation of second-sound resonances. The transmitters and receivers consisted of four mylar strips 2 mm wide, 20 μm thick set 90° apart on the inner wall of the stator, parallel to the rotation axis. The mylar strips were aluminized on the outside and held to insulating electrodes by a 200 V bias voltage.

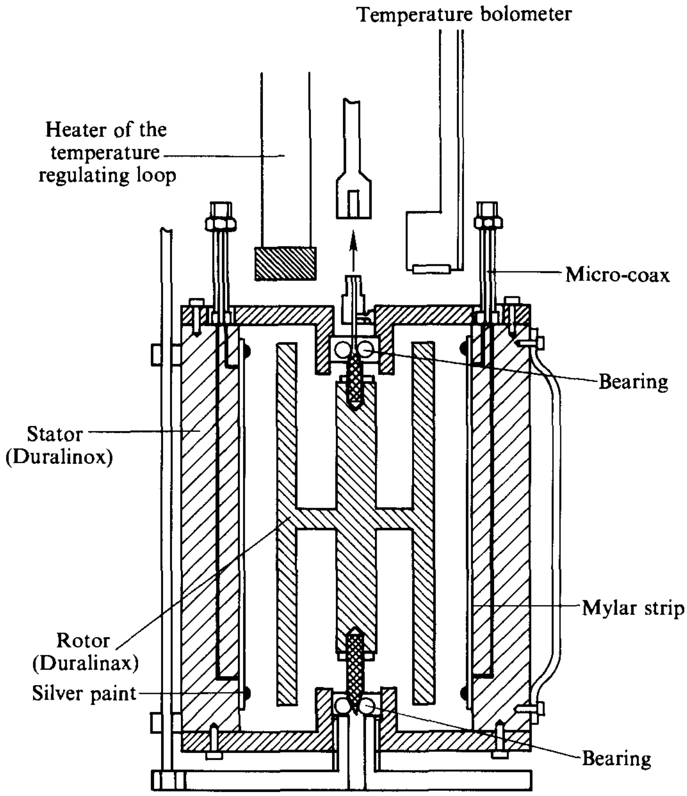

FIGURE 20. Second-sound attenuation apparatus constructed by Wolf *et al.* (1981). Resonances of second sound were obtained principally in the azimuthal direction from the mylar strips attached to the outer cylinder. Other transducers at the top and bottom allowed axial attenuation to be obtained.

They were excited by a 1–10 V r.m.s. a.c. signal of angular frequency ω. Second sound was generated by the oscillatory motion of the superfluid behind the strips, the normal fluid being relatively less mobile because of its viscosity.

The principal resonances observed in this apparatus were purely orthoradial (azimuthal) modes where the temperature oscillation, at least in the low d/R limit, varies as

$$T = T_0 \exp[\mathrm{i}(\omega t - m\phi)], \tag{4.4}$$

where ϕ is the azimuthal angle. At higher frequencies, radial resonances were seen with $\lambda = d = 2d/p$, where p is an integer for a pure radial mode and λ is the wavelength. Weak axial resonances also appeared.

The authors measured the attenuation of second sound by observing the Q-values of their resonances. The Q in the absence of attenuation, Q_0, is typically 5000 for $d = 0.575$ cm. Rotation induces a Doppler splitting of the resonance into two components, plus broadening of the resonances owing to attenuation of second sound by the vortices.

The apparatus was also equipped with resistance elements at the top and bottom of the cylinders in order to allow a study of the attenuation of second-sound pulses in the axial direction. Attenuation of a radial mode could occasionally be observed at high rotation rates.

For a given vortex-line density (length of line per unit volume) described by

$L(\boldsymbol{r}, \theta)$ at the point $\boldsymbol{r}$, oriented at an angle with $\boldsymbol{k}$ ranging between θ and $\theta + d\theta$, they assumed the attenuation of second sound in a given direction of propagation $\boldsymbol{k}$ is given by

$$\alpha(\boldsymbol{k}, \boldsymbol{r}) = \frac{B\kappa}{4u_2} \int L(\boldsymbol{r}, \theta) \sin^2\theta \, d\theta. \tag{4.5}$$

Measurement of the components of attenuation in different directions could be assumed to allow information on $L(\boldsymbol{r}, \theta)$ to be gathered.

The authors attempted to get some idea of the average velocity profile of the superflow by analysing the Doppler shifts of their resonant peaks. This was complicated by the presence of the mylar strips which gave a splitting of the resonances even in the absence of rotation. Their results appear to show that the mean velocity profile of the superfluid has the classical value given by (1.2) even at rotation rates (5 revs/s) which correspond to a highly turbulent state of the fluid. There are not many classical measurements of the profile in turbulent flow: Taylor (1936), however, has reported detailed velocity profile measurements for a rotating outer cylinder.

Experiments on second-sound attenuation of an azimuthal mode are shown in figure 21 (*a*, *b*) for a relatively wide gap $d = 0.575$ cm. Here we see the attenuation rising with breaks between which the attenuation can be approximated by straight lines. The critical velocities are called Ω_0, Ω_1, $\Omega_2, \ldots$ and correspond to our Ω_0, $\Omega_{1c}, \Omega_{2c}, \ldots$. The authors report that the number of thresholds increases with d, with 3 for $d = 0.08$ cm and 0.15 cm, 4 for $d = 0.35$ cm and 5 for $d = 0.575$ cm. Figure 22 (*a*, *b*) shows the attenuation for $d = 0.08$ cm, where the first break Ω_0 (figure 22 *b*) is interpreted by the authors as corresponding to the first appearance of vortices in the gap.

The authors report a systematic investigation of these thresholds as a function of both temperature and gap size. They find that Ω_1 and Ω_2 have a weak temperature dependence, but Ω_3 is strongly temperature dependent. Ω_2 disappears below 1.8 K.

The authors suggest that Ω_0 corresponds to the appearance of an 'alley' of vortices in the annulus of density $n(\Omega_0) = 1/d^2$. They then argue that Ω_0 varies inversely with d which explains why Ω_0 is clearly visible only at low values of d. (We advance a theory of the appearance of vortices in the gap in §4.8 below.)

The observation that the mean velocity profile is consistent with (1.2) then prompts the authors to argue that between Ω_0 and Ω_1, $v_n = v_s$ and that a uniform array of vortices appears in the channel as demonstrated by Bendt (§4.5). If the array is uniform then the attenuation of second sound between Ω_0 and Ω_1 should theoretically be linear in Ω with a slope calculable from simple mutual friction theory. The observed attenuation is found to agree with the expected value. The observed ratio of these quantities gave an average of 0.92 ± 0.2 over a range of gap sizes from 0.08 cm to 0.575 cm and 1.65 K to 2.12 K.

The authors calculate the ratio of the observed critical angular velocity Ω_1 to Ω_T, the theoretical critical angular velocity for the uncoupled normal fluid, by comparison with the critical Taylor number for narrow gap for the normal fluid alone:

$$Ta_c = 2R_1 d^3 \left(\frac{\Omega_T}{\nu_n}\right)^2 \approx 3400. \tag{4.6}$$

They find Ω_1/Ω_T, averaged over temperature, ranges from 5 at $d = 0.08$ cm to 35 at $d = 0.575$ cm. They conclude that the vortices, by coupling the two components, stabilize the normal fluid. This observation appears to confirm qualitatively the predictions of Chandrasekhar & Donnelly (1957).

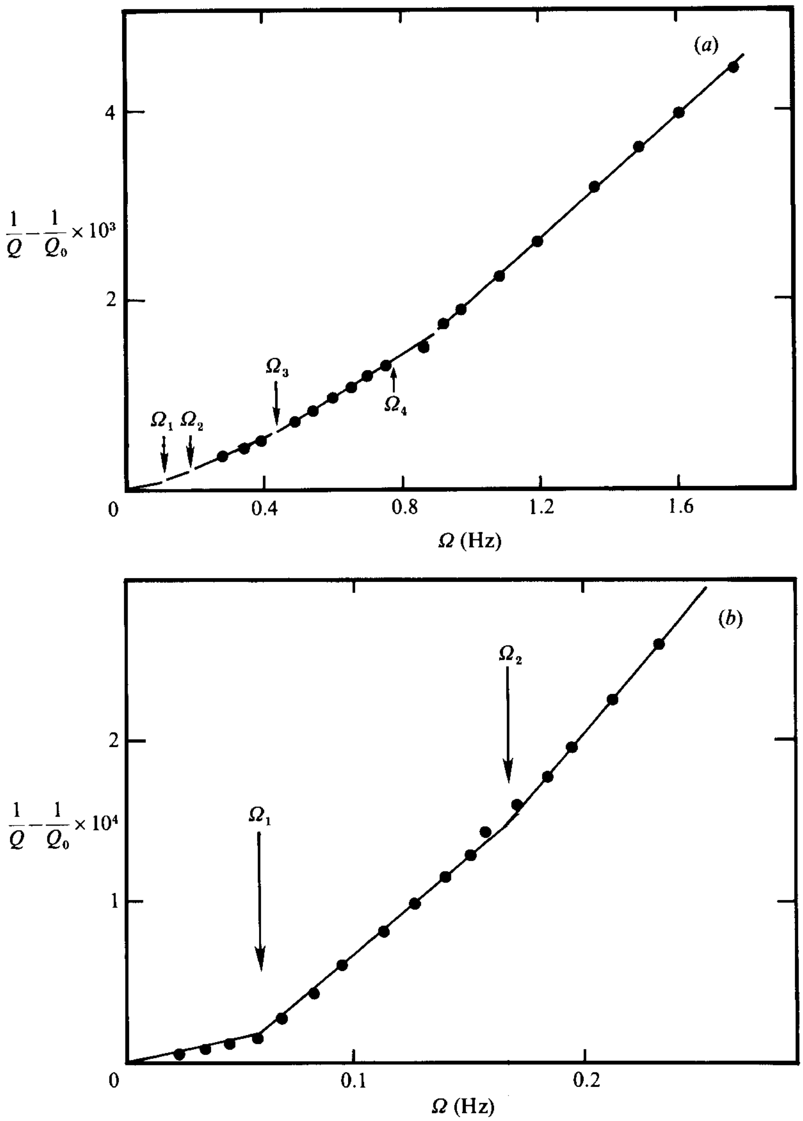

FIGURE 21. (a) Second-sound attenuation measured in the azimuthal direction by the resonant cavity method. Here $R_1 = 2.075$ cm, $R_2 = 2.65$ cm, $d = 0.575$ cm and $T = 1.99$ K. The detailed figure (b) does not show a region of zero attenuation.

Some results for $d = 5.75$ mm are reported showing that the axial attenuation is greater than the transverse attenuation above Ω_3, suggesting that the vortices are disorganized, and possibly anisotropic.

The authors note that Ω_1 and Ω_2 are independent of temperature and may be instabilities of the superfluid, while Ω_3 is strongly temperature dependent and perhaps is connected with an instability of the normal fluid. They attempt to correlate Ω_1 with the Mamaladze–Matinyan criterion (see §4.9 below), but find that their data lie two orders of magnitude higher. Their critical velocities Ω_0 are also much higher than those observed by Donnelly (table 3), Snyder (table 5), and Heikkila & Hollis Hallett (table 2). They are also much higher than a theoretical estimate which we give in §4.9 below. These comparisons suggest that the authors'

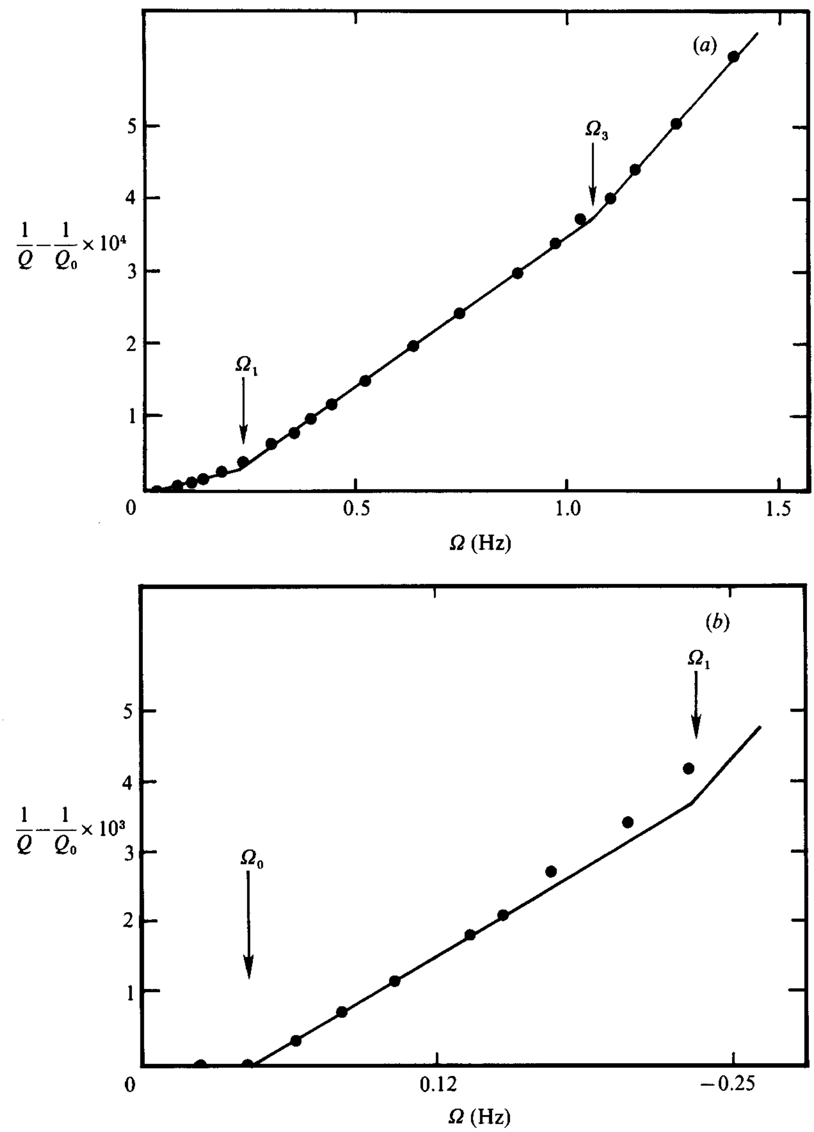

FIGURE 22. (*a*) Second-sound attenuation measured in the azimuthal direction by the resonant cavity method. $R_1 = 2.57$ cm, $R_2 = 2.65$ cm, $d = 0.08$ cm, $T = 1.86$ K. The authors suggest that the first appearance of vortices can be seen in the detailed plot (*b*), $D_{1c0} = 1660$ (see table 6).

attenuation sensitivity was not sufficient to observe the first entry of vortices in the annulus.

It appears that it would be well worth repeating these interesting measurements with more sophisticated second-sound attenuation techniques such as are used for modern counterflow turbulence research (Swanson 1985). The cylinders in this research were not well designed for end effects, and observations of radial attenuation were actually done in a different apparatus.

4.8. *Entry of vortices between rotating cylinders*

The results on the first quanta of circulation and first entry of vortices in a uniformly rotating annulus were obtained by powerful free-energy minimization techniques,

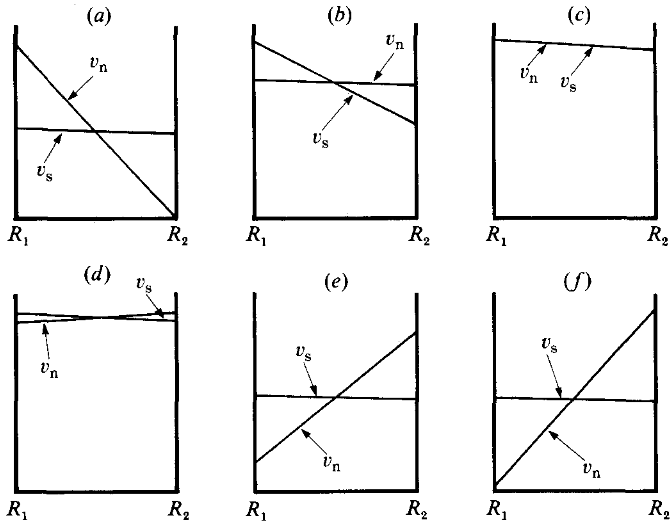

FIGURE 23. Distribution of flow of the two fluids in the annulus between concentric cylinders in the absence of quantized vortex lines; $\eta = 0.95$. The distribution of the normal fluid is given by (1.2) and the superfluid is in potential flow arranged to match the normal-fluid velocity in the middle of the gap. The cases are given for six different values of μ: (a) $\mu = 0$ (the inner cylinder rotating); (b) 0.5; (c) 0.9025 (potential flow); (d) 1 (solid-body rotation); (e) 5; (f) 100. $\mu = \infty$ corresponds to the outer cylinder rotating.

discussed in the papers by Fetter (1966, 1967) and Stauffer & Fetter (1968). When $\Omega_1 \neq \Omega_2$, the normal fluid is in shearing motion, and one would no longer expect the methods of equilibrium thermodynamics to be applicable. We shall explore in this section some ideas on vortex arrays that might appear at low rates of rotation in the presence of shear.

We take our starting point from the discussion of the rotating annulus by Donnelly & Fetter (1966), referred to briefly in §3.2 above. Although the discussion concerned equilibrium flow in an annulus, strictly speaking there is relative motion of the normal and superfluids. To appreciate this one has only to examine figure 23. The velocity distributions of figure 23 are drawn on the following assumptions. The normal-fluid velocity is distributed according to (1.2) which is the sum of solid-body-rotation and potential-flow terms. By analogy with the ideas of Donnelly & Fetter (1966), the superfluid acquires circulation $\Gamma = 2\pi\Omega_1 R^2$ to match the velocity of the normal fluid midway between cylinders, and is otherwise distributed in potential flow, $v_s = \Gamma/2\pi r$ within the annulus. Thus even in the solid-body rotation treated by Donnelly & Fetter ($\mu = 1$), there is relative motion between normal and superfluid components, despite the fact that the normal fluid is free of shear.

If we follow this hint from Donnelly & Fetter, we might speculate that in general vortices will appear when their presence can minimize the relative velocity between the two fluids, and ignore the shear motion of the normal fluid. A simple argument suggests how this might occur. For $\mu > \eta^2$, we have $A > 0$ and the vorticity $\omega = 2A > 0$. A single row of vortices in the annulus will provide an increase in superfluid velocity $\kappa/2\pi d$ tending to bring v_s toward v_n. So a criterion for this to occur would be (for $R_1 \approx R_2$)

$$\left.\begin{aligned} \Omega_2 R_2 - v_s = \Omega_2 R_2 - \frac{\Gamma}{2\pi R_2} &\geqslant \frac{\kappa}{\pi d} \\ \text{or} \qquad D_2 - D_1 \geqslant \frac{R_2}{\pi d} \quad &(A > 0). \end{aligned}\right\} \tag{4.7}$$

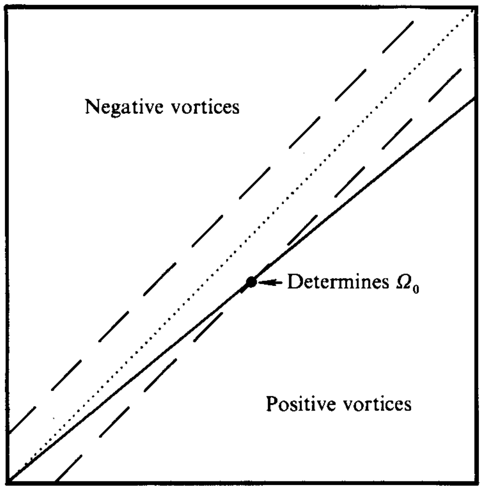

FIGURE 24. Boundaries indicated by dashed lines according to (4.9) for the entry of positive and negative vortices in the annulus between rotating cylinders. Potential flow is shown by the dotted line. The solid line corresponds to solid-body rotation, $\Omega_1 = \Omega_2$, or $D_1 = D_2\eta^2$. The intersection of the solid-body rotation and the criterion for entry of positive vortices reproduces Ω_0 of §§3.2 and 3.3 above. There are no vortices in the region between dashed lines according to these ideas.

For $\mu < \eta^2$, we have $A < 0$ and vorticity $\omega = 2A < 0$. A single row of vortices in the annulus will provide a decrease in superfluid velocity $\kappa/\pi d$ tending to bring v_s down toward v_n. Then the criterion would become

$$\left.\begin{aligned} v_s - \frac{\kappa}{\pi d} &\geqslant \Omega_2 R_2 \\ \text{or} \qquad D_1 - D_2 &\geqslant \frac{R_2}{\pi d} \quad (A < 0). \end{aligned}\right\} \tag{4.8}$$

Building on the qualitative argument just given, Swanson & Donnelly (1987) have shown that the minimum free energy for vortices in a general flow between rotating cylinders is obtained by minimizing the average of $\rho_s(v_s - v_n)^2$. They find that a single row of vortices appears when $|A| > \kappa L/\pi d^2$ where the logarithmic factor $L = \ln(2d/\pi a)$, and a second row when $|A| > 1.85\,\kappa L/\pi d^2$. They argue that this relation is valid anywhere in the (D_1, D_2)-plane, that is, even for counter-rotating cylinders. In our notation their criterion reads

$$|D_2 - D_1| > \frac{(R_2 + R_1)\ln(2d/\pi a)}{\pi d}. \tag{4.9}$$

Equation (4.9) defines the boundaries for the entry of vortices in the annulus. These are shown by the dashed lines in figure 24. Thus the primary (i.e. unperturbed) state in the lower triangle contains positive vortices, and the primary state in the upper triangle contains negative vortices. Along the dotted potential-flow line and indeed between dashed lines, no vortices enter the annulus.

Solid-body rotation is indicated by the solid line in figure 24, i.e. $D_1 = D_2\eta^2$. When this criterion is combined with (4.9), we find the condition for entry of vortices in an annulus in solid-body rotation is

$$\Omega_2 \geqslant \frac{\kappa}{\pi d^2}\ln\left(\frac{2d}{\pi a}\right) = \Omega_0, \tag{4.10}$$

which recovers (3.7) for Ω_0.

4.9. *Stability theories*

Mamaladze & Matinyan (1963) recognized that if the flow of helium II between concentric cylinders involves an array of vortices, the tension in these vortices themselves would provide a restoring force for a displaced element of fluid. They then argued that the Rayleigh criterion would be modified in the direction of extra stability.

Their calculations proceeded in the same spirit as those of Lord Rayleigh (cf. Chandrasekhar 1961, §§66, 67). The situation is considered at absolute zero where there is no viscosity. They assumed that the vortex lines in the annulus are dense enough to allow continuum calculations, and assumed further that the distribution of the superfluid velocity is that of a viscous fluid (see (1.2)). They used the equation of motion of the rotating superfluid first advanced by Hall (1960)

$$\frac{\partial \boldsymbol{v}_s}{\partial t}+(\boldsymbol{v}_s\cdot\boldsymbol{\nabla})\boldsymbol{v}_s+\nu_s\left[\boldsymbol{\omega}\times\operatorname{curl}\left(\frac{\boldsymbol{\omega}}{\omega}\right)\right]=-\frac{1}{\rho}\boldsymbol{\nabla}p, \tag{4.11}$$

$$\operatorname{div}\boldsymbol{v}=0,$$

$$u_r=0 \quad \text{at } r=R_1 \text{ and } R_2,$$

where $\nu_s=\epsilon/\rho_s\kappa$, ϵ being the tension (energy per unit length) of a vortex filament, $\epsilon=\frac{1}{2}\rho_s\kappa^2\ln(d/a)$. Making small perturbations about the equilibrium state, they derived a stability criterion which they suggested should replace Rayleigh's for helium II.

Recently, Barenghi & Jones (1987) have reconsidered the stability problem in the light of the experiments discussed in this paper. They have begun their work by examining the effect of vortex tension in the pure superfluid: the problems of finite temperature, including vortex tension, mutual friction and normal fluid viscosity are quite complicated.

Barenghi & Jones note first that Mamaladze & Matinyan failed to realize that A can be positive or negative depending on Ω_1 and Ω_2 (see figure 24). Thus their equations for the perturbed velocities are not correct. In addition, Barenghi & Jones allow for non-axisymmetric perturbations: Mamaladze & Matinyan, following Chandrasekhar & Donnelly assumed that the first modes to become unstable are axisymmetric. Barenghi & Jones find that when the inner cylinder rotates, the onset of non-axisymmetric modes occurs at a lower velocity than for axisymmetric modes, and these long-wavelength axial modes reduce the critical velocity to zero. Further they find that non-axisymmetric modes of long wavelength can be unstable when the outer cylinder is rotating, in qualitative agreement with our conclusion of §4.4. The situation at finite temperature will be expected to involve the normal fluid, which will select the azimuthal and axial wavenumbers for which the flow is unstable with lowest D_1 and D_2.

4.10. *Discussion and outlook*

A rotating-cylinder viscometer is an absolute instrument for determining shear viscosity. The instability phenomena described here show that for helium II the design of such an instrument, which must be sensitive enough to reach the stable flow region, is restricted by the requirement for reaching the very low velocities of either cylinder for stable flow. These problems are described by us in a further paper (Donnelly & LaMar 1987).

The method of finding the equilibrium distribution of circulation and vortices in a rotating container has usually been investigated by free-energy minimization. Owing to the circumstances that Couette flow is a combination of solid-body rotation and potential flow, we have shown that free-energy methods may be extended to general flows between rotating cylinders to find the equilibrium state even in the presence of shear.

When the cylinders are rotating sufficiently slowly the normal fluid will be in Couette flow and the superfluid in potential flow (except perhaps for end effects). At some critical rotation rate, quantized vortices enter the flow. An experimental investigation by second-sound attenuation should establish whether our arguments in §4.8 and the specific result of Swanson & Donnelly (1987) given by (4.9) are correct. Note that (4.9) should be valid for the cases in which outer and inner cylinders are rotating in the same or opposite directions.

The more challenging problem of finding the stability of the states just discussed is evolving rapidly. On the theoretical side it appears that it will now be profitable to try to solve the full equations of motion for the stability of the flow of helium II. One important problem will be whether the average number of vortices N_v across the gap will be large enough to justify treating the vortices as a continuum. We see from the tables that N_v can be as small as 3. The choice of gap size will influence this problem, and an instability calculation at finite temperatures would be of further assistance in selecting an experimental design. On the experimental side, there is every indication that second-sound attenuation will prove to be a powerful tool in exploring the modes of instability in the flow between concentric rotating cylinders. In doing so, the complications mentioned in §1.3 in studying classical flows shold be kept in mind. Allowable ramping rates, preferred aspect ratios, optimum end conditions and multiplicity of states should be carefully investigated as they may be considerably different in the flow of helium II than in classical flows.

Once instability sets in, it is not clear how much information on the resulting nonlinear flow can be obtained by second-sound attenuation. Here again, the rotating-cylinder viscometer may become a powerful tool for further progress and insight. Such an instrument would be a fitting continuation of the tradition established a century ago by Mallock and Couette.

Looking even further ahead, the experiments discussed here are capable of interesting variations. Temperature gradients between the top and bottom of the cylinders (the Kapitza experiment of §2.1), or between the inner and outer cylinders will alter the basic state and create new phenomena for study. There is much to be gained from such a study: the two-fluid theory of helium II with rotation and vortices present has had much theoretical but limited experimental attention. The study of the stability of such flows is perhaps the most rigorous test of the validity of the equations of motion and boundary conditions one can devise.

We are grateful to Paul Roberts, Charles Swanson, Christopher Jones and Carlo Barenghi for comments on a draft of this paper. We are also grateful to Charles Swanson, Carlo Barenghi and Christopher Jones for their new calculations. This research was supported by the National Science Foundation Low Temperature Physics Program under grant DMR 83-13487 and the Fluid Mechanics Program under grant MSM 81-17569.

REFERENCES

ANDERECK, C. D., LIU, S. S. & SWINNEY, H. L. 1986 Flow regimes in a circular Couette system with independently rotating cylinders. *J. Fluid Mech.* **164**, 155–183.

BARENGHI, C. F., DONNELLY, R. J. & VINEN, W. F. 1983 Friction on quantized vortices in helium II. *J. Low Temp. Phys.* **52**, 189–247.

BARENGHI, C. F. & JONES, C. A. 1987 On the stability of superfluid helium between rotating concentric cylinders. (preprint).

BEARDEN, J. A. 1939 A precision determination of the viscosity of air. *Phys. Rev.* **56**, 1023–1040.

BENDT, P. J. 1966 Instability of helium II potential flow between rotating cylinders. *Phys. Rev. Lett.* **17**, 680–682.

BENDT, P. J. 1967*a* Attenuation of second sound in helium II between rotating cylinders. *Phys. Rev.* **153**, 280–284.

BENDT, P. J. 1967*b* Superfluid flow transition in rotating narrow annuli. *Phys. Rev.* **164**, 262–267.

BENDT, P. J. & DONNELLY, R. J. 1967 Threshold for superfluid vortex lines in a rotating annulus. *Phys. Rev. Lett.* **19**, 214–216.

BENJAMIN, T. B. 1978*a* Bifurcation phenomena in steady flows of a viscous liquid. I. Theory. *Proc. R. Soc. Lond.* A **359**, 1–26.

BENJAMIN, T. B. 1978*b* Bifurcation phenomena in steady flows of a viscous liquid. II. Experiments. *Proc. R. Soc. Lond.* A **359**, 27–43.

BENJAMIN, T. B. & MULLIN, T. 1981 Anomalous modes in the Taylor experiment. *Proc. R. Soc. Lond.* A **377**, 221–249.

BENJAMIN, T. B. & MULLIN, T. 1982 Notes on the multiplicity of flows in the Taylor experiment. *J. Fluid. Mech.* **121**, 219–230.

BURKHALTER, E. & KOSCHMIEDER, E. L. 1973 Steady supercritical Taylor vortex flow. *J. Fluid Mech.* **58**, 547–560.

CHANDRASEKHAR, S. 1961 *Hydrodynamic & Hydromagnetic Stability*. Clarendon Press.

CHANDRASEKHAR, S. & DONNELLY, R. J. 1957 The hydrodynamic stability of helium II between rotating cylinders I. *Proc. R. Soc. Lond.* A **241**, 9–28.

COUETTE, M. M. 1888 Sur un nouvel appareil pour l'étude du frottement des fluides. *Comptes Rendus* **107**, 388–390.

COUETTE, M. M. 1890 Etudes sur le frottement des liquides. *Ann. Chem. Phys.* VI, **21**, 433–510.

CRAWFORD, G. L., PARK, K. & DONNELLY, R. J. 1985 Vortex pair annihilation in Taylor wavy-vortex flow. *Phys. Fluids* **28**, 7–9.

DI PRIMA, R. C. & SWINNEY, H. L. 1981 Instabilities and transition in flow between concentric rotating cylinders. In *Hydrodynamic Instabilities and the Transition to Turbulence* (ed. H. L. Swinney & J. P. Gollub), pp. 139–180. Springer.

DONNELLY, R. J. 1958 Experiments on the stability of viscous flow between rotating cylinders. *Proc. R. Soc. Lond.* A **246**, 312–325.

DONNELLY, R. J. 1959 Experiments on the hydrodynamic stability of helium II between rotating cylinders. *Phys. Rev. Lett.* **3**, 507–508.

DONNELLY, R. J. & FETTER, A. L. 1966 Stability of superfluid flow in an annulus. *Phys. Rev. Lett.* **17**, 747–750.

DONNELLY, R. J. & FULTZ, D. 1960 Experiments on the stability of viscous flow between rotating cylinders II. Visual observations. *Proc. R. Soc. Lond.* A **258**, 101–123.

DONNELLY, R. J. & LAMAR, M. M. (1987) Absolute measurement of the viscosity of classical and quantum fluids by rotating viscometers. *Phys. Rev.* A**36** (in press).

DONNELLY, R. J., PARK, K., SHAW, R. & WALDEN, R. W. 1980 Early nonperiodic transitions in Couette flow. *Phys. Rev. Lett.* **44**, 987–989.

DONNELLY, R. J. & SWANSON, C. E. 1986 Quantum turbulence. *J. Fluid Mech.* **173**, 387–429.

ELLEAUME, P., HULIN, J. P. & PERRIN, B. 1978 Hydrodynamic instabilities in the rotating Couette flow of superfluid helium. *J. Phys. Paris* **39**, C**6** 163–164.

FETTER, A. L. 1966 Equilibrium distribution of rectilinear vortices in a rotating container. *Phys. Rev.* **152**, 183–189.

FETTER, A. L. 1967 Low-lying superfluid states in a rotating annulus. *Phys. Rev.* **153**, 285–296.

FEYNMAN, R. P. 1955 Application of quantum mechanics to liquid helium. In *Progress in Low Temperature Physics*, vol. I (ed. C. J. Gorter), pp. 17–53. North-Holland.

GLABERSON, W. I. & DONNELLY, R. J. 1986 Structure, distributions and dynamics of vortices in helium II. In *Progress in Low Temperature Physics*, vol. IX (ed. D. F. Brewer), pp. 3–142, North-Holland.

HALL, H. E. 1960 The rotation of liquid helium II. *Adv. Phys.* **9**, 89–146.

HALL, H. E. & VINEN, W. F. 1955 Non-linear dissipative processes in liquid helium II. *Phil. Mag.* **46**, 546–548.

HEIKKILA, W. J. & HOLLIS HALLETT, A. C. 1955 The viscosity of liquid helium II. *Can. J. Phys.* **33**, 420–435.

HOLLIS HALLETT, A. C. 1953 Experiments with a rotating cylinder viscometer in liquid He II. *Proc. Camb. Phil. Soc.* **49**, 717–727.

JEONG, K. 1986 Instability of flow states in Taylor–Couette geometries. PhD thesis, University of Oregon.

JONES, C. A. 1981 Nonlinear Taylor vortices and their stability. *J. Fluid Mech.* **102**, 249–261.

KAPITZA, P. L. 1941 The study of heat transfer in Helium II. *J. Phys. USSR* **4**, 181–210.

KOLM, H. H. & HERLIN, M. A. 1956 New method for measuring the absolute viscosity of liquid helium II. *Phys. Rev.* **102**, 607–613.

LONDON, F. 1954 *Superfluids* Vol. 2. Wiley.

MALLOCK A. 1888 Determination of the viscosity of water. *Proc. R. Soc. Lond.* **13**, 126–133.

MALLOCK, A. 1895 Experiments on fluid viscosity. *Phil. Trans. R. Soc. Lond.* A **187**, 41–56.

MAMALADZE, YU. G. & MATINYAN, S. G. 1963 Stability of rotation of a superfluid liquid. *Sov. Phys. JETP* **17**, 1424–1425.

MULLIN, T. 1982 Mutations of steady cellular flows in the Taylor experiment. *J. Fluid. Mech.* **121**, 207–218.

ONSAGER, L. 1949 Statistical hydrodynamics. *Nouvo Cim. Suppl.* **6**, 279–287.

OSBORNE, D. V. 1950 The rotation of liquid helium II. *Proc. Phys. Soc.* A **63**, 909–912.

PARK, K., CRAWFORD, G. L. & DONNELLY, R. J. 1981 Determination of transition in Couette flow in finite geometries. *Phys. Rev. Lett.* **47**, 1448–1450.

PARK, K. & DONNELLY, R. J. 1981 Study of the transition to Taylor vortex flow. *Phys. Rev.* A **24**, 2277–2279.

PARK, K. & JEONG, K. 1985 Transition measurements near a multiple bifurcation point in a Taylor–Couette flow. *Phys. Rev.* A 31, 3457–3459.

SNYDER, H. A. 1969 Wave-number selection at finite amplitude in rotating Couette flow. *J. Fluid Mech.* **35**, 273–298.

SNYDER, H. A. 1974 Rotating Couette flow of superfluid helium. In *Proc. 13th Intl. Conf. Low Temp. Phys. LT13* vol. 1, pp. 283–287. Plenum.

STAUFFER, D. & FETTER, A. L. 1968 Distribution of vortices in rotating helium II. *Phys. Rev.* **168**, 156–159.

SWANSON, C. E. 1985 A study of vortex dynamics in counterflowing helium II. Ph.D. thesis, Department of Physics, University of Oregon.

SWANSON, C. E. & DONNELLY, R. J. 1987 Appearance of vortices in Taylor–Couette flow of helium II. *J. Low Temp. Phys.* **67**, 185–193.

SWANSON, C. E., WAGNER, W. T., BARENGHI, C. F. & DONNELLY, R. J. 1987 Calculation of frequency & velocity dependent mutual friction parameters in helium II. *J. Low Temp. Phys.* **66**, 263–276.

TAYLOR, G. I. 1923 Stability of a viscous liquid contained between two rotating cylinders. *Phil. Trans. R. Soc. Lond.* A **223**, 289–343.

TAYLOR, G. I. 1936 Fluid friction between rotating cylinders II – distribution of velocity between concentric cylinders when the outer one is rotating and inner one is at rest. *Proc. R. Soc. Lond.* A **157**, 565–578.

TOUGH, J. T. 1982 Superfluid turbulence. In *Progress in Low Temperature Physics*, Vol. 8 (ed. D. F. Brewer), pp. 133–219. North-Holland.

Vinen, W. F. 1961 The detection of a simple quantum of circulation in liquid helium II. *Proc. R. Soc. Lond.* A **260**, 218–236.

Wheeler, R. G., Blakewood, C. H. & Lane, C. T. 1955*a* Second sound attenuation in rotating helium II. *Phys. Rev.* **99**, 1667–1672.

Wheeler, R. G., Blakewood, C. H. & Lane, C. T. 1955*b* Second sound attenuation in rotating helium II. *Phys. Rev.* **98**, 1196.

Wolf, P. E., Perrin, B., Hulin, J. P. & Elleaume, P. 1981 Rotating Couette flow of helium II. *J. Low Temp. Phys.* **44**, 569–593.